Orbit-Spin Coupling and Variations in the Length of the Hale Cycle

James H. Shirley

Torquefx
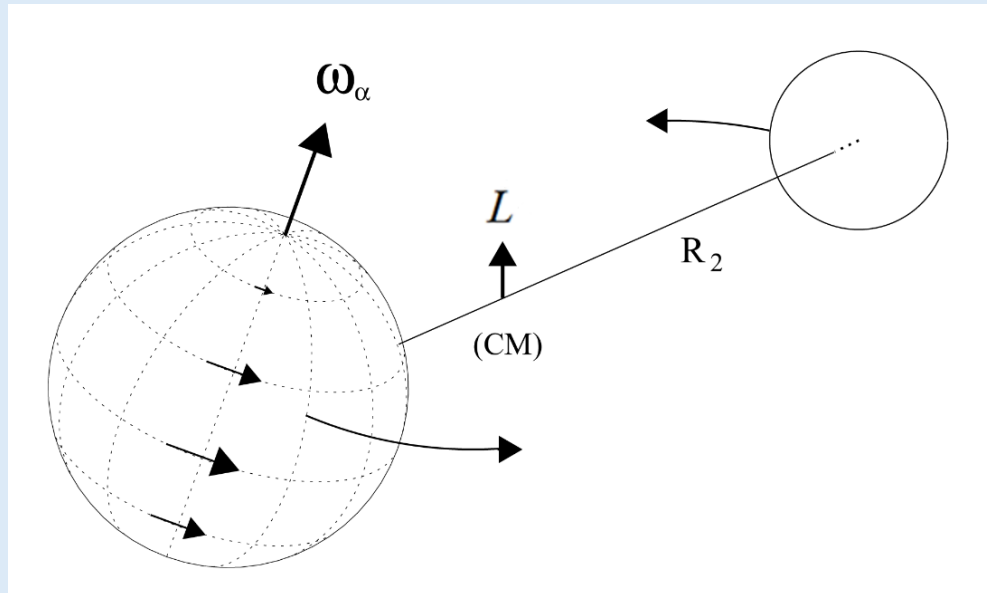Simi Valley, California, USA
jrocksci@att.net

19th MHD Days, Liebnitz Institute for Astrophysics, Potsdam

2 December 2024

"…the solar velocity field has to be sufficiently well reproduced first, before one should expect success in reproducing the dynamo."

Käpylä et al., 2023, Simulations of solar and stellar dynamos and their theoretical interpretation, Space Science Reviews 219:58 (2023)

The Orbit-Spin Coupling Hypothesis

- *Momentum sourced from solar system orbital motions is deposited within the circulating fluid envelopes of the Sun and planets by means of a **reversing torque***

- This torque is entirely separate and distinct from known tidal mechanisms and precession

- From an orbital dynamics point of view, the transferred momentum lies "down in the noise." The momentum deposited may nonetheless be surprisingly large, and potentially important, in relation to solar and geophysical processes. There is plenty of momentum down there!

- *For perspective*: The orbiting Sun routinely gains and loses angular momentum equivalent to the *total orbital angular momentum* of the *terrestrial planets*, on cycle times ranging from 15-26 years

Solar System Angular Momenta		
Quantity:	Angular Momentum	Percent
Solar System Total	3.15×10^{43} kg m^2 s^{-1}	100
Orbit of Jupiter	1.90×10^{43} kg m^2 s^{-1}	60.3
Orbit of Saturn	7.83×10^{42} kg m^2 s^{-1}	24.9
Orbit of Neptune	2.51×10^{42} kg m^2 s^{-1}	8
Orbit of Uranus	1.74×10^{42} kg m^2 s^{-1}	5.5
Outer Planets Total:	3.11×10^{43} kg m^2 s^{-1}	98.7
Orbit of Earth + Moon	2.68×10^{40} kg m^2 s^{-1}	0.09
Orbit of Venus	1.85×10^{40} kg m^2 s^{-1}	0.06
Orbit of Mars	3.53×10^{39} kg m^2 s^{-1}	0.01
Orbit of Mercury	9.10×10^{38} kg m^2 s^{-1}	0.003
Inner planets Total:	4.97×10^{40} kg m^2 s^{-1}	0.158
Solar Barycentric Revolution	< 0 to > 4.60×10^{40} kg m^2 s^{-1}	< = 0.15
Rotation of the Sun	1.92×10^{41} kg m^2 s^{-1}	0.61

The "coupling term acceleration" is given by:

$$CTA = -c\left(\dot{L} \times \omega_\alpha\right) \times r$$

Here L (or dL/dt) is the time rate of change of the orbital angular momentum, ω_α is the angular velocity of rotation, and r is a position vector. The coupling efficiency coefficient c is to be determined through a comparison of modeling outcomes with observations

This identifies a global-scale acceleration field:

- Axial rotation carries the body "through" the field

- The accelerations are tangential to a spherical surface with radius r

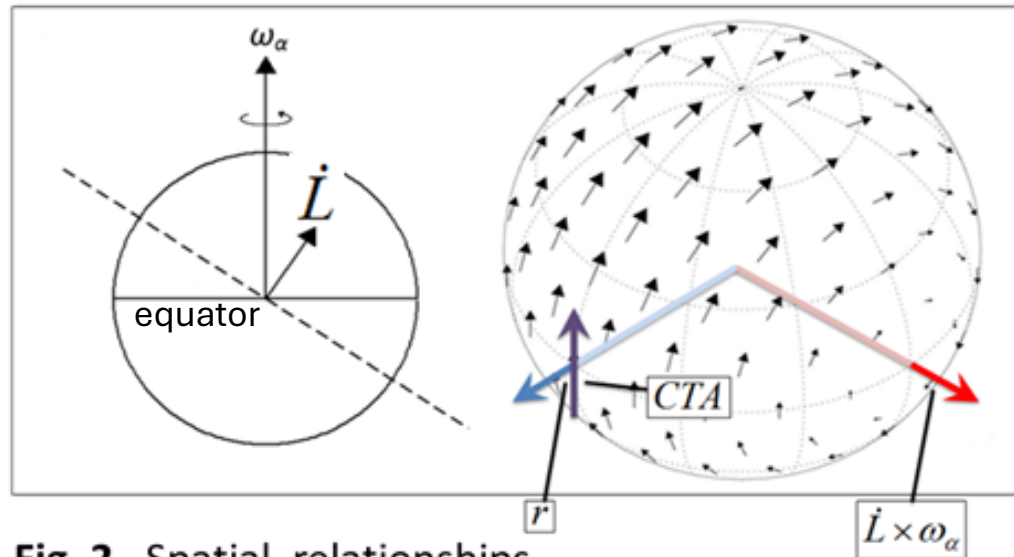- Meridional accelerations dominate in equatorial latitudes

**Fig. 2.** Spatial relationships

- The *orbit-spin coupling hypothesis* predicts cycles of intermittent intensification and relaxation of large-scale flows in solar and planetary atmospheres

- The coefficient c quantifies the fractional portion of the orbital momentum that may participate in the excitation of solar-physical and geophysical phenomena

- A formal derivation of the coupling equation may be found in *Shirley* (2017)

The *forcing function* and the *torque*

- Dash-dotted blue curve: Solar *dL/dt* due to giant planets only

- Solid blue curve: Solar *dL/dt* due to all planets; fine structure mainly results from synodic cycles of inner planets with outer planets

- Torque: Northward acceleration at 90 E in the rotating heliographic system (Time step: 1 day; cycle time ~1 CR)

- ***Inner planet contributions to solar motion yield pulses of the torque amplitude***
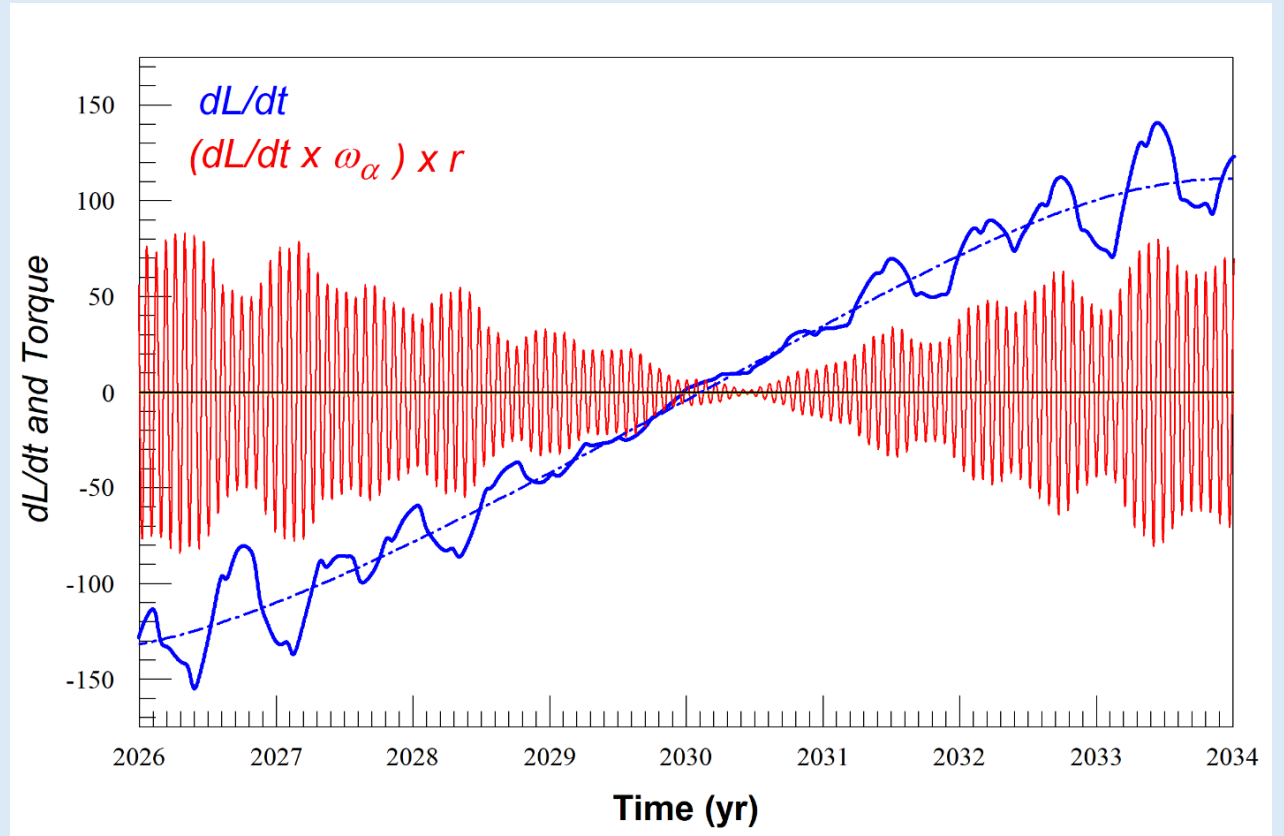

The upcoming torque reversal of 2030 accompanies a close approach by the Sun to the solar system barycenter, termed "PERIBAC"
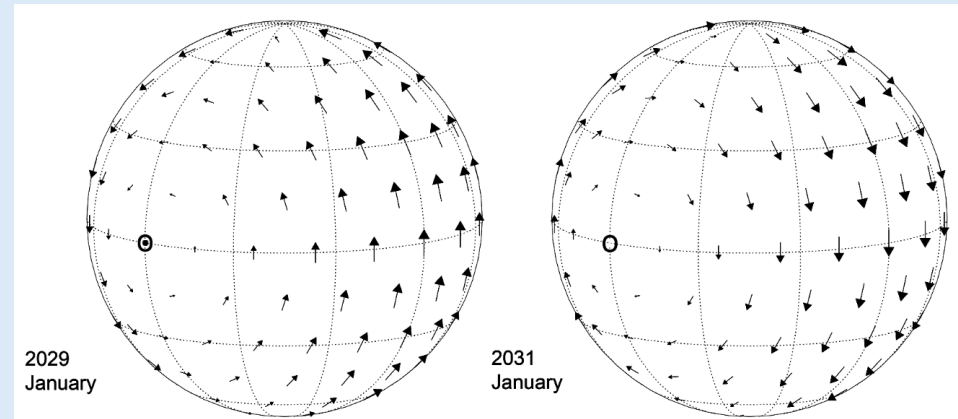
Orbit-spin Coupling Torques and Near-Surface Meridional Flows (1)

A direct test of the orbit-spin coupling hypothesis (Shirley, 2017) employed SOHO-MDI derived near-surface meridional flow speeds in the years 1996-2009 (Hathaway & Rightmire, 2010)
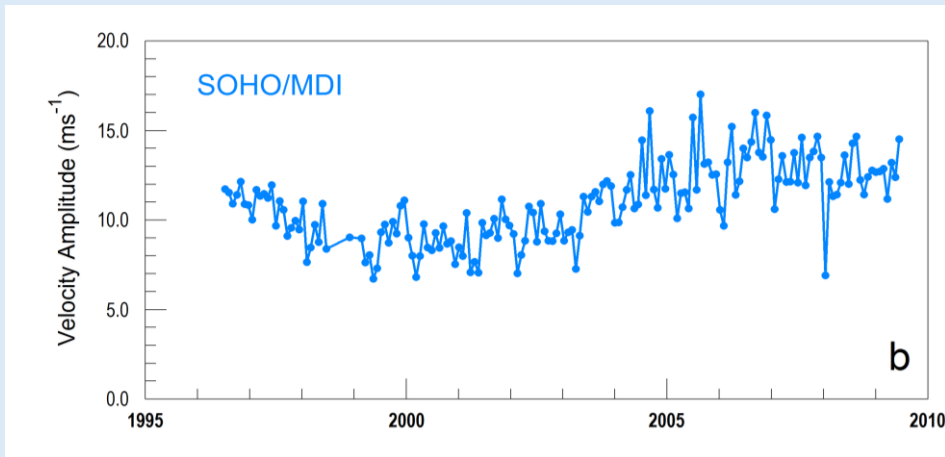
Variations in the Sun's Meridional Flow over a Solar Cycle

DAVID H. HATHAWAY AND LISA RIGHTMIRE   Authors Info & Affiliations

🔒 CHECK ACCESS

Solar Meridional Flow
Abstract
References and Notes
eLetters (0)

Solar Meridional Flow

The surface of the Sun is composed of plasma that exhibits observable flow patterns. The weakest flow pattern occurs along meridional lines from the equator toward the poles. **Hathaway and Rightmire** (p. 1350) measured the meridional flow using observations taken with the Michelson Doppler Imager onboard the Solar and Heliospheric Observatory between 1996 and 2009 and found that meridional flow varied with the solar cycle, such that flow was faster during the 2004–2009 minimum than during the 1996–1997 minimum. This finding provides further evidence that the last solar minimum was peculiar by comparison with previous cycles.
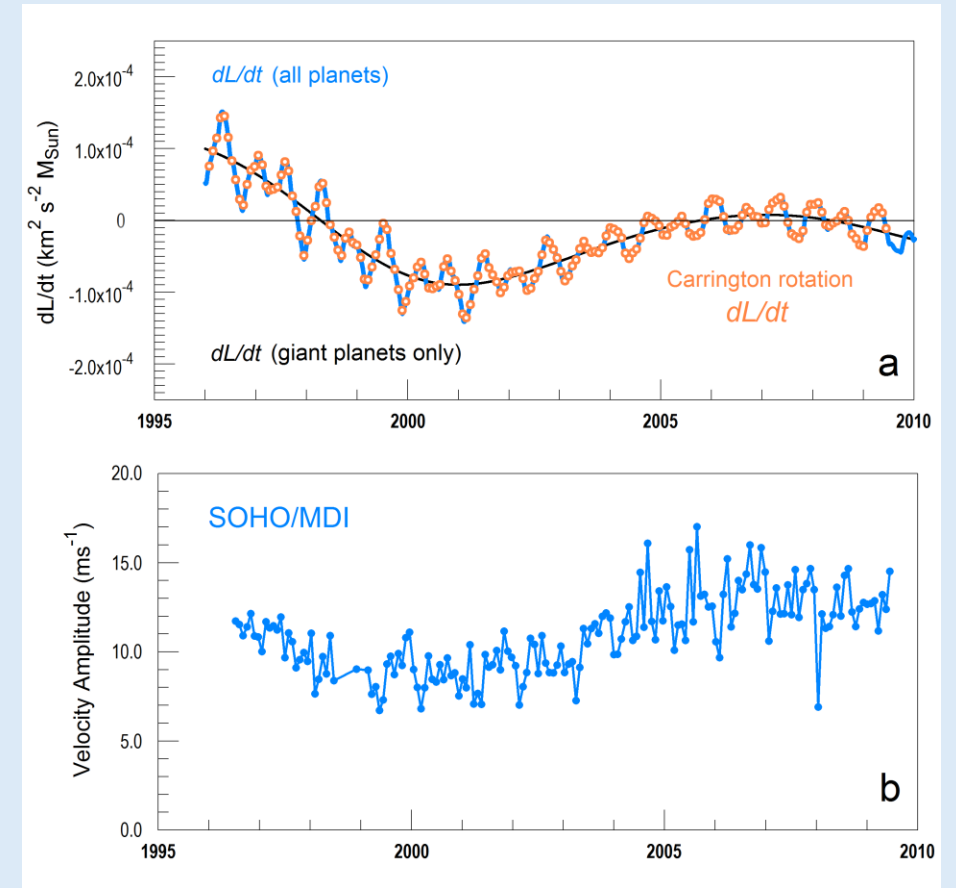
Orbit-spin Coupling Torques and Near-Surface Meridional Flows (2)

The unlagged correlation of the flow velocities curve and *dL/dt, each* sampled with time steps of one Carrington Rotation, is significant at the 99.9% level

Lag	HR 2010 : Giant Planets		HR 2010 : JPL Horizons (all planets)	
(Carrington rotations)	*r*	*p*	*r*	*p*
0	**0.520**	< 0.001	0.438	< 0.001
1	0.503	< 0.001	0.436	< 0.001
2	0.485	< 0.001	0.443	< 0.001
3	0.468	< 0.001	**0.458**	< 0.001
4	0.449	< 0.001	0.451	< 0.001
5	0.430	< 0.001	0.415	< 0.001
6	0.415	< 0.001	0.376	< 0.001

Correlation coefficients are likewise significant at the 99.9% level for lags ranging between 1 and 6 Carrington rotations

(a): The dynamical forcing function *dL/dt*.

(b): SOHO/MDI time series of solar meridional flow speeds of small magnetic features (Hathaway & Rightmire 2010).

Orbit-spin Coupling Torques and Near-Surface Meridional Flows (3)

The detrended series also exhibit significant correlations

Panel C compares normalized, detrended time series of meridional flows and *dL/dt* with meridional flows lagged by 4 CR. The probability for the lag-4 correlation is *p*=0.011

| Lag	HR 2010 : Giant Planets		HR 2010 : JPL Horizons (all planets)		HR 2010 : JPL Horizons (Detrended)	
(Carrington rotations)	*r*	*p*	*r*	*p*	*r*	*p*
0	**0.520**	< 0.001	0.438	< 0.001	0.060	0.221
1	0.503	< 0.001	0.436	< 0.001	0.015	0.432
2	0.485	< 0.001	0.443	< 0.001	0.056	0.236
3	0.468	< 0.001	**0.458**	< 0.001	0.159	0.020
4	0.449	< 0.001	0.451	< 0.001	**0.177**	**0.011**
5	0.430	< 0.001	0.415	< 0.001	0.105	0.088
6	0.415	< 0.001	0.376	< 0.001	0.036	0.322

Meridional motions of small magnetic features in Cycle 23 track the rate of change of the Sun's orbital angular momentum *dL/dt* - with a lag of ~4 months
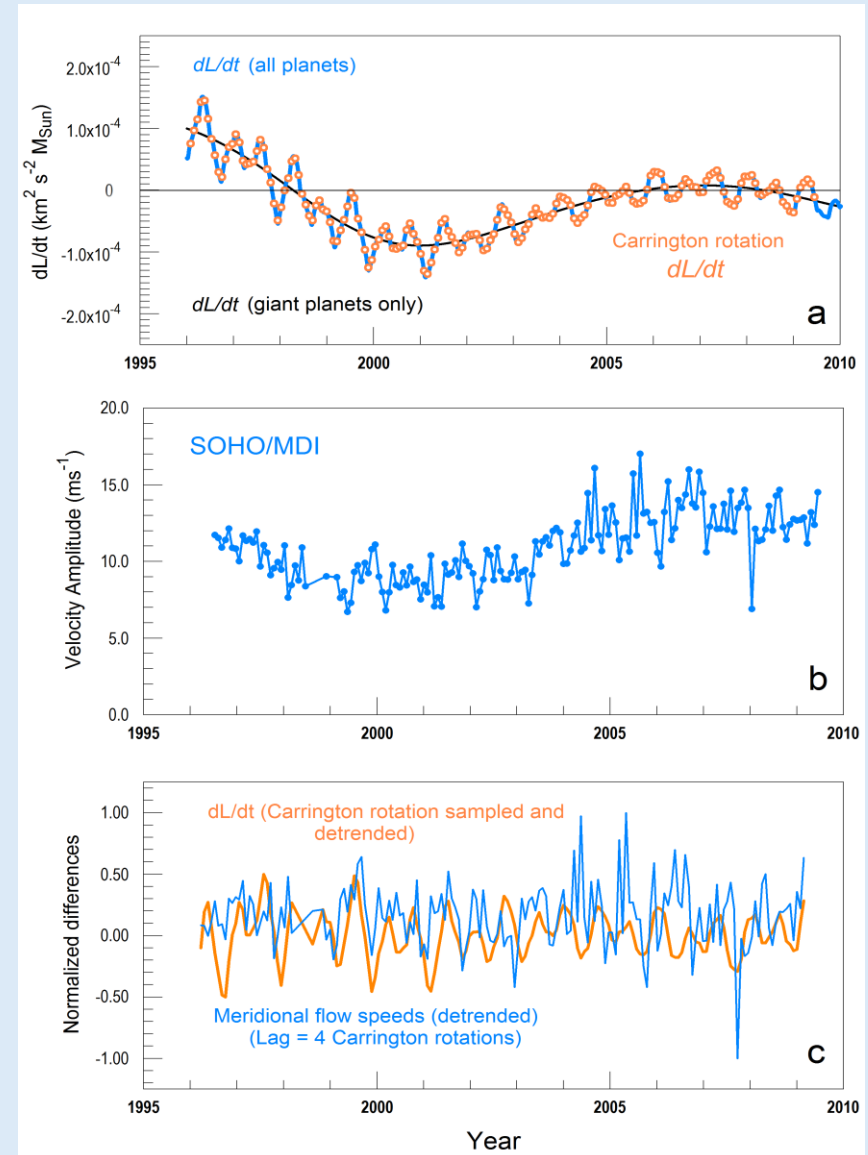
Barycentric Orbital Motion and the Hale Cycle:
Recognizing Two Modes

Three-Body Mode: When Uranus and Neptune are near opposition, their effects approximately cancel. The Sun's resulting (3-body) "trefoil" trajectory is comparatively regular and symmetric
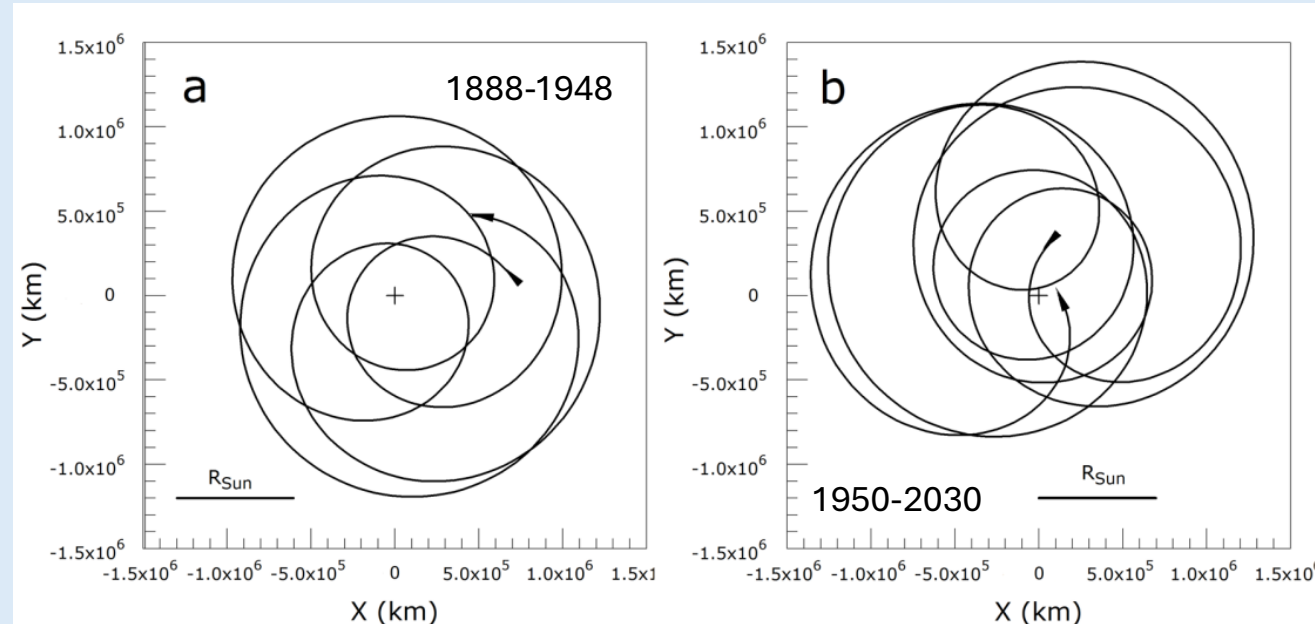

Five-Body Mode: At other times, perturbing effects of U and N produce a more asymmetric (5-body) trajectory with larger displacements and more complex ("disordered") phasing

The above polar plots illustrate the motion of the center of the Sun with respect to the solar system barycenter (+) for two intervals of interest. The radius of the Sun is shown in each panel to provide scale. Motion is plotted relative to the J2000 ecliptic coordinate frame. a): 1888-1948. Smaller and larger loops alternate to form a relatively regular and symmetric pattern. b): 1950-2030. An azimuthally *asymmetric* pattern is formed, with the Sun traveling both much closer to the barycenter, and much farther from the barycenter, at different times, in comparison with a).

Hale Cycle and Schwabe Cycle characteristics differ significantly between these two modes

# 3-body Mode: Dynamical and Solar Magnetic Cycles in Phase

1891-1951
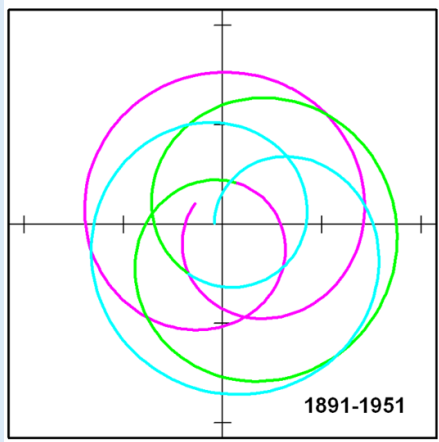
- Three barycentric orbital cycles correspond to three Hale magnetic cycles

- Six ~10-year "pulses" of the torque amplitude correspond in time to six ~10-yr Schwabe cycles

- Lagging of the SSN curve with respect to dynamical forcing in Cycle 16 "recovers" in 17 and 18
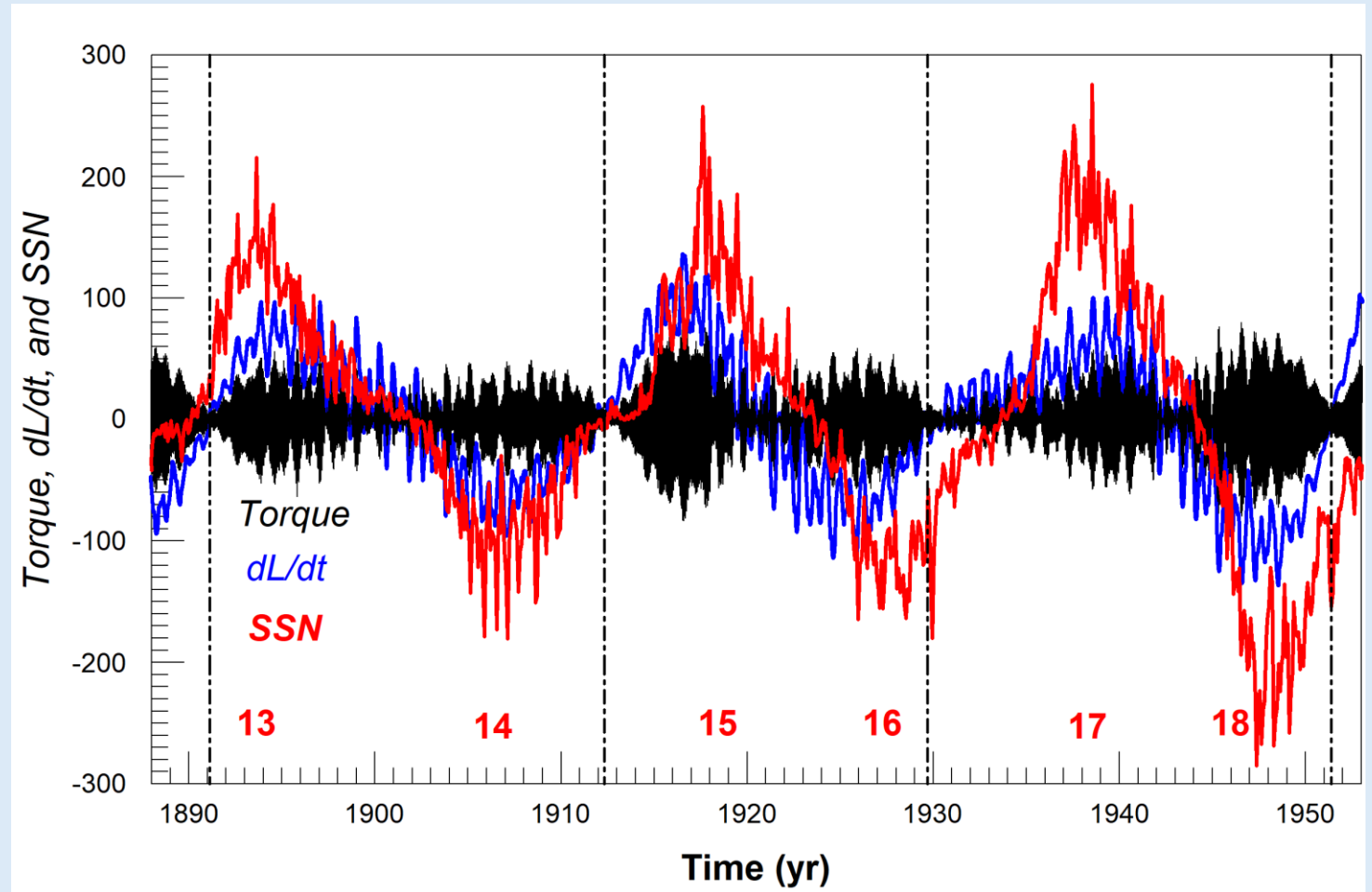
The orbit-spin coupling forcing function (*dL/dt*, in blue), together with scaled orbit-spin coupling surface accelerations *cta* (in black), in juxtaposition with Hale cycle (magnetic polarity included) SIDC solar sunspot numbers (red) in the years 1888-1953 (WDC-SILSO, Royal Observatory of Belgium, Brussels). **Vertical broken lines identify the times of closest approach by the Sun to the solar system barycenter.**

Regularization of Schwabe Cycle periods in the 1891-1951 3-body motion episode has been recognized, but physical explanations remain speculative
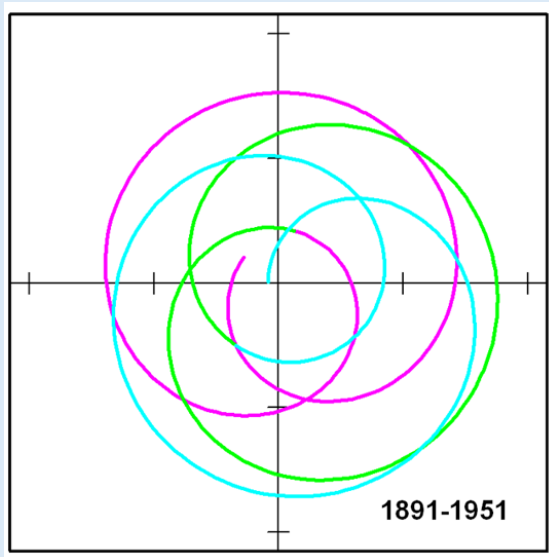
1891-1951

A review of the solar cycle length estimates

R. E. Benestad

Meteorological Institute, Oslo, Norway

[1] New estimates of the solar cycle length are calculated from an up-to-date monthly sunspot record using a novel but mathematically rigorous method involving multiple regression, Fourier approximation, and analytical expressions for the first derivative based on calculus techniques. The sensitivity of the estimates to smoothing are examined and the analysis is used to identify possible systematic changes in the sun. The solar cycle length analysis indicates a pronounced change in the sun around 1900, before which the estimates fluctuate strongly and after which the estimates show little variability. There have been

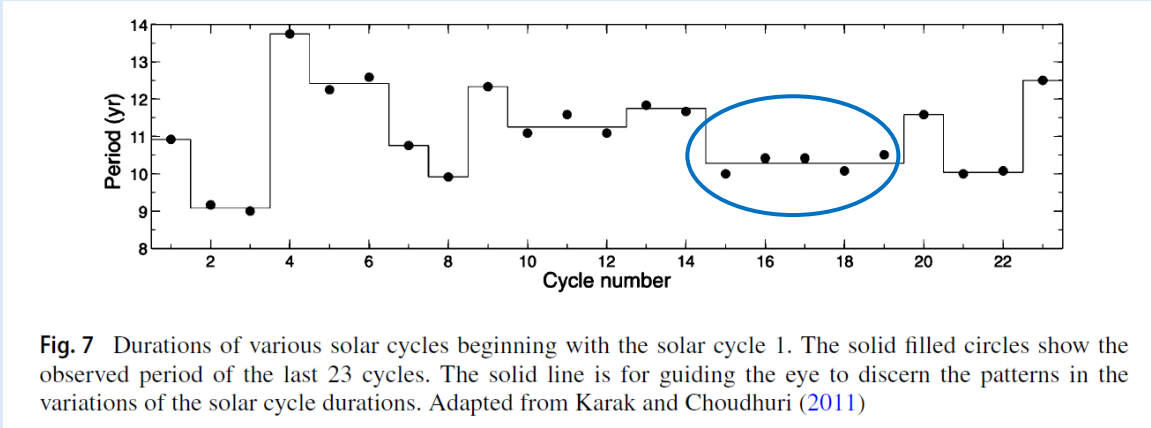which they are based was flawed [*Damon and Laut*, 2004; *Laut*, 2003].

[4] There is a number of different ways to estimate the solar cycle length [*Solanki and Fligge*, 2002; *Solanki et al.*, 2002], from estimating the time interval between successive maxima, successive minima, to wavelet anaysis. Sometimes, the sunspot values at solar max is noisy and not well-defined (Figure 1) making it difficult to estimate the time of maximum. Here a new method is introduced, involving a truncated Fourier representation of the sunspot record and using the cosine series to solve for the first and
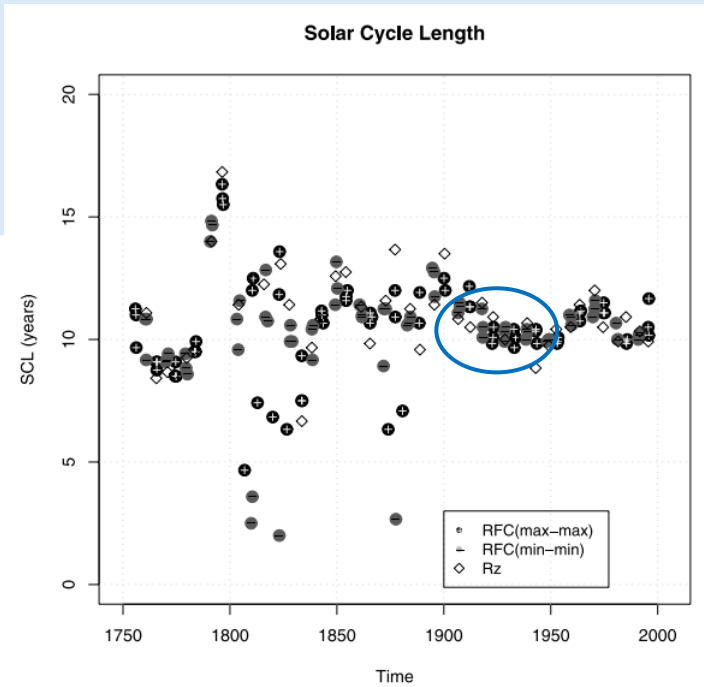
Figure 2. Solar Cycle length estimates derived from the RFC-method (circles) and from taking the maxima and minima directly from the monthly Wolf sunspot number (diamonds). For the RFC-results, black symbols marked with "+" represent maxima and grey symbols with "−"


Fig. 7 Durations of various solar cycles beginning with the solar cycle 1. The solid filled circles show the observed period of the last 23 cycles. The solid line is for guiding the eye to discern the patterns in the variations of the solar cycle durations. Adapted from Karak and Choudhuri (2011)

"…cycles 15 -19 had an almost constant period somewhat shorter than 11 yr, suggesting a stronger meridional circulation at that time."

Hazra et al., 2023, Space Science Reviews 219:39

Phasing of the dynamical and magnetic cycles is similar during the two most recent 3-Body episodes:

Peribac	Cycle Time	Hale Start Date	Cycle Time
1712.137		1712	
	21.301		21.5
1733.438		1733.5	
	18.09		21.9
1751.528		1755.4	
	21.054		20.1
1772.582		1775.5	
	20.148 +/- 1.787		21.167 +/- 0.95
1891.126		1890.123	
	21.191		22.501
1912.317		1912.624	
	17.382		21.334
1929.699		1933.958	
	21.679		20.497
1951.378		1954.455	
	20.084 +/- 2.353		21.44 +/- 1.01
Combined:	20.116 +/- 1.869		21.31 +/- 0.87

3-Body Hale cycle durations average **21.3 yr**
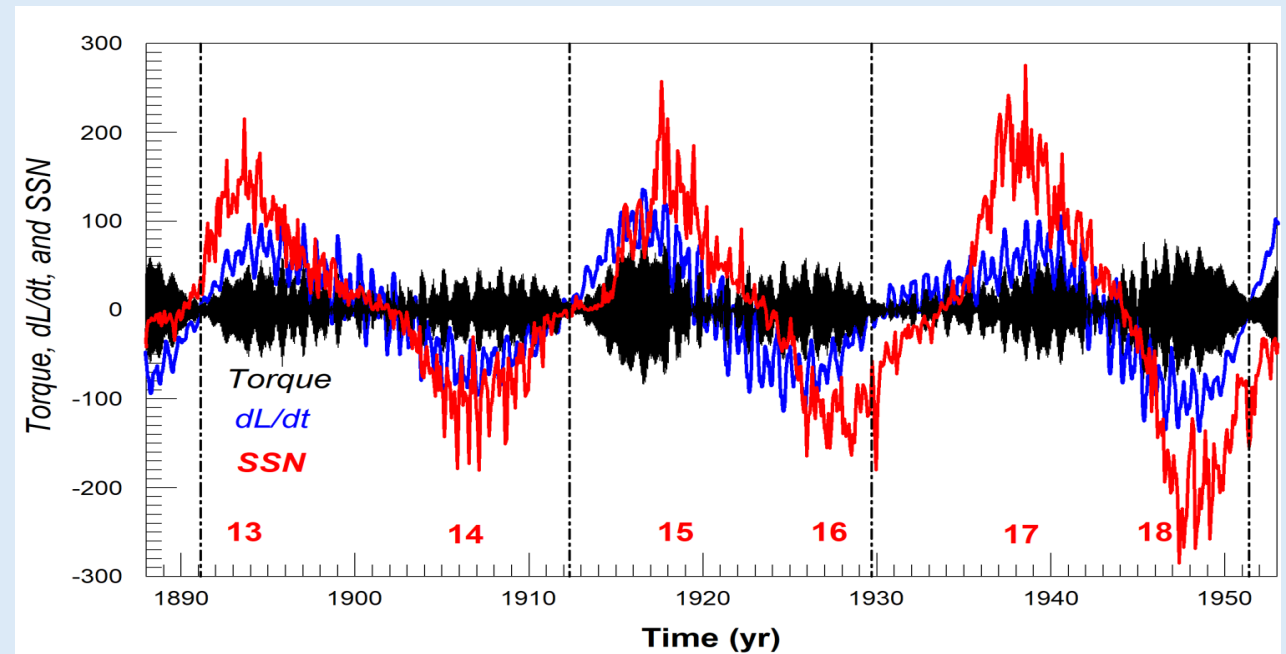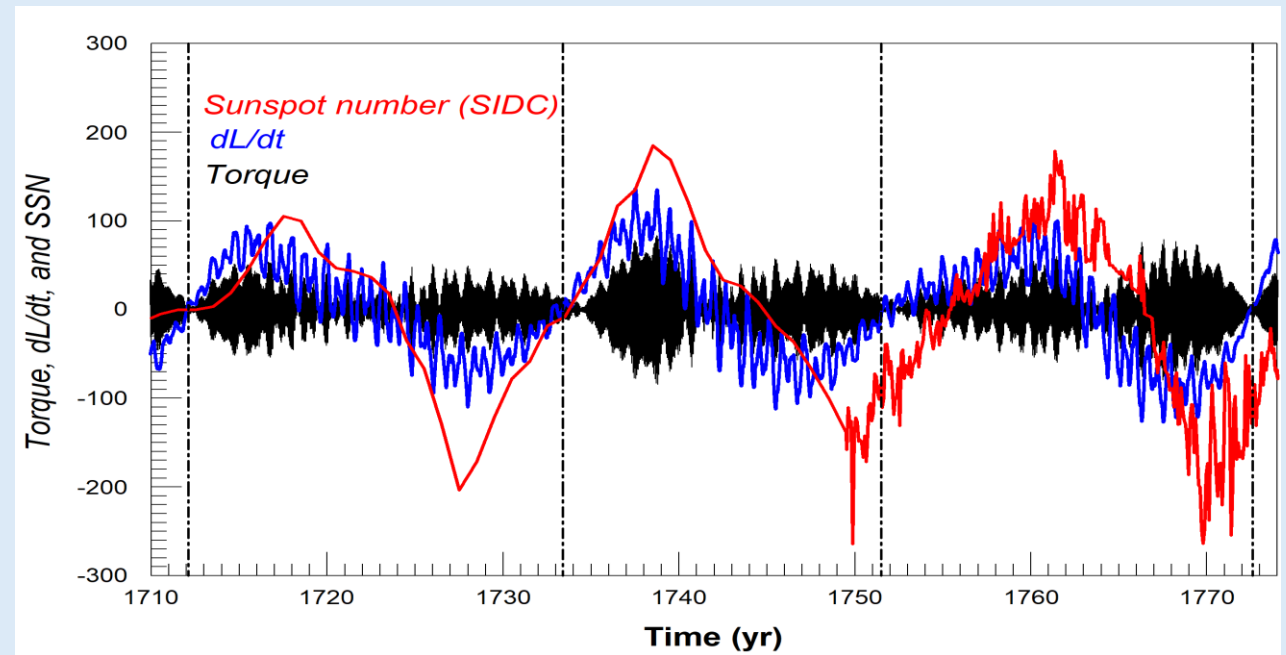
Jose (1965) documented a recurrence interval of length ~179 yr in the barycentric orbital motion of the Sun

Eight 179-yr cycles of the orbital radius vector **R** are shown at right for the interval from 816 (CE) to 2069

Each "Jose Cycle" consists of 9 individual orbits defined by close approach epochs ("peribacs"). Single orbit cycles are of mean duration 19.86 yr

Red ellipses identify the most recent episodes >

The synodic period of Uranus and Neptune (~171 yr) largely dictates the timing of the 3-body episodes. Thus, *the phasing of these episodes drifts slowly with respect to the Jose cycle*
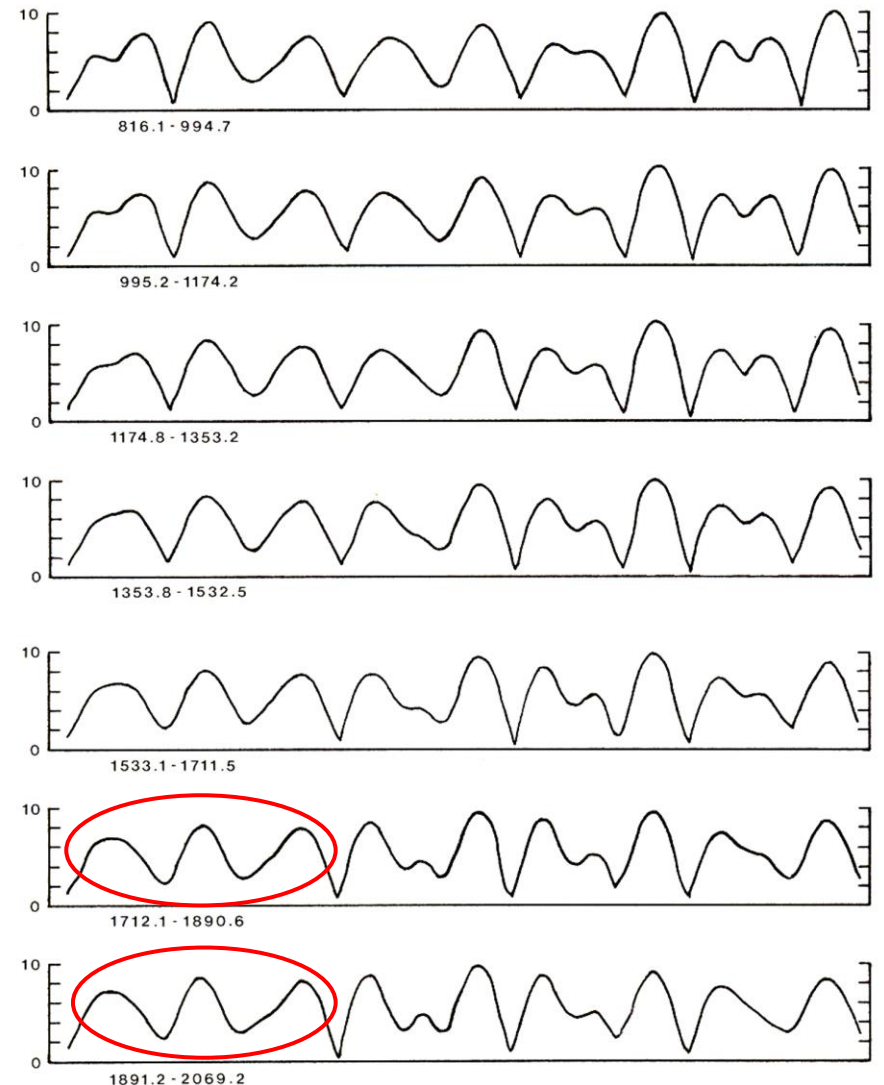

Fig. 3. The 179-yr cycle of the solar barycentric orbit radius R over 7 cycles beginning in A.D. 816. Units are 10^{-3} AU. The time-period in calendar years for each curve is noted. Successive close approaches to the barycenter (minima of the curve) define the starting and ending points of individual solar orbits of Figures 1 and 2.

Fairbridge, R. W., and Shirley, J. H. 1987. Prolonged Minima and the 179-yr Cycle of the Solar Inertial Motion, Sol. Phys. 100, 191.

5-body Mode: Magnetic cycle lags dynamical cycle

6 orbit cycles = 5 Hale magnetic cycles
of mean duration ~23 years

| Peribac	Cycle Time	Hale Start Date	Cycle Time
1772.582			
	23.568	1775.538	
1796.150			22.833
	15.283	1798.371	
1811.433			25
	23.666	1823.371	
1835.099			20.167
	15.781	1843.538	
1850.879			23.504
	22.693	1867.042	
1873.573			23.081
	17.553	1890.123	
1891.126			
	19.757 +/- 3.977		22.917 +/- 1.752
	^		

Alternating longer, and shorter, orbital cycles:
("Whiplash")

The solar dynamo: A damped, driven oscillator...?
(Wilmot-Smith et al., 2006)
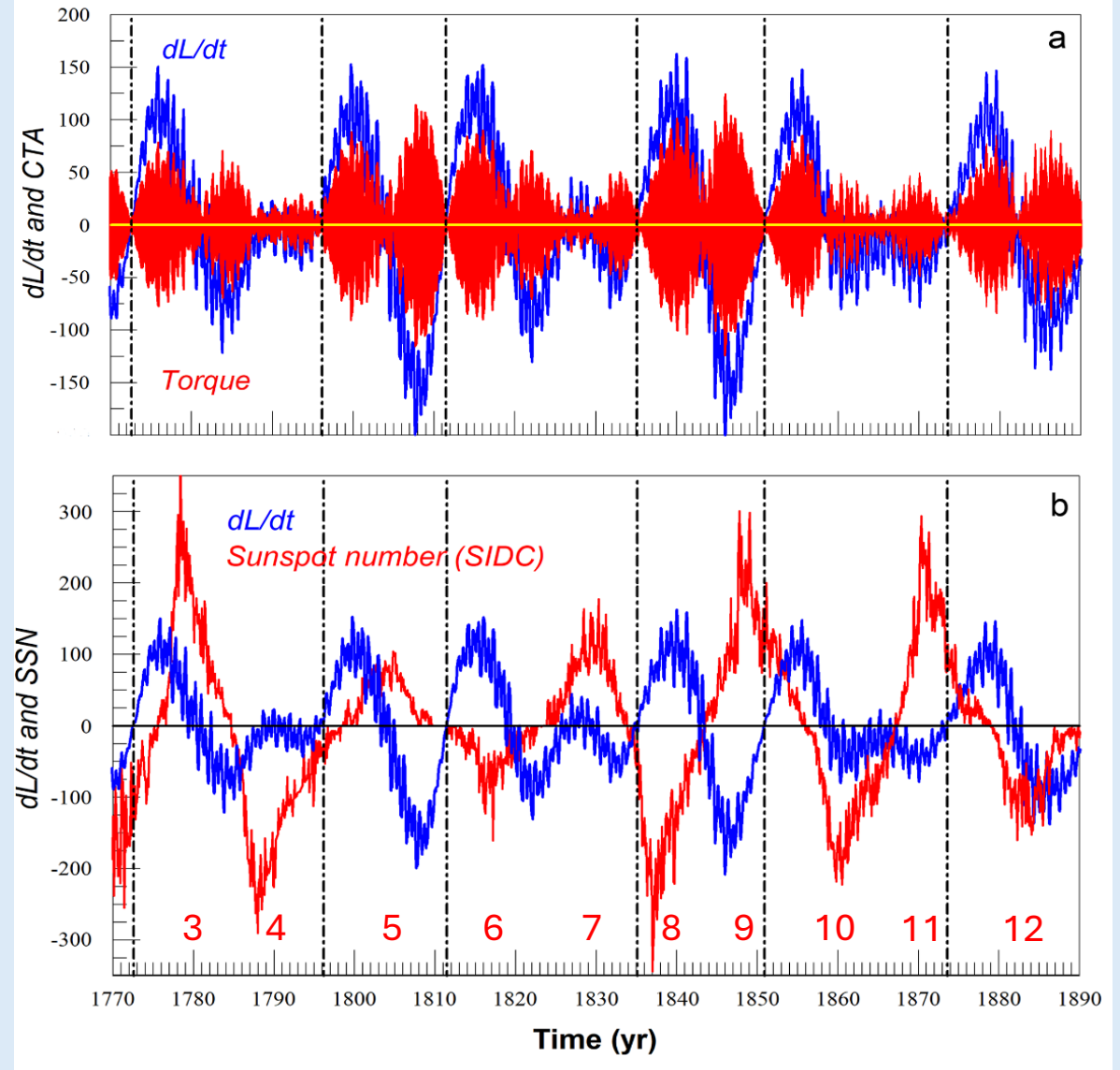
The orbit-spin coupling forcing function (*dL/dt*) (in blue) (a), together with orbit-spin coupling surface accelerations (*cta*), and (b) in juxtaposition with monthly SSN in the years 1770-1890 (WDC-SILSO). Vertical broken lines identify peribacs.

Time Delay Effects and System Memory (1)
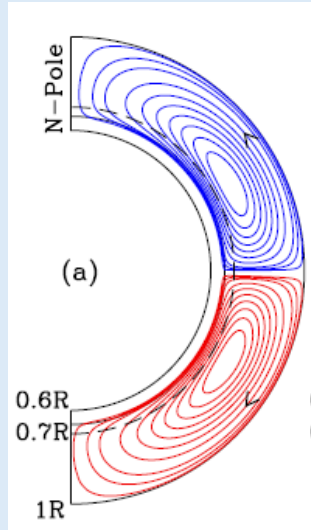
(Belucz & Dikpati, 2013)

- Meridional circulations in the Sun have been characterized as a sort of conveyor belt, returning flux from the surface to the base of the CZ

- Finite circulation speeds introduce a time delay, providing 'system memory' (Wilmot-Smith et al., 2006)

- We additionally recognize that meridional circulation cells may **store and release momentum sourced from orbital motions**

  (Shirley, 2017: Time Dependent Theory of Solar Meridional Flows, arXiv:1706.01854)

Journal of Geophysical Research: Planets   10.1029/2019JE006077
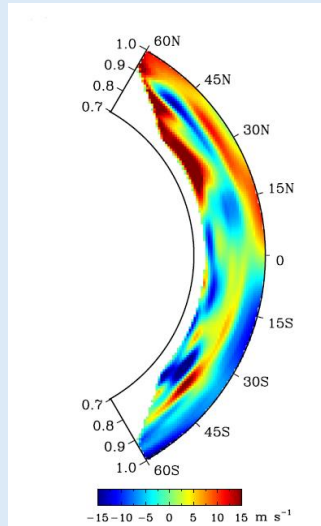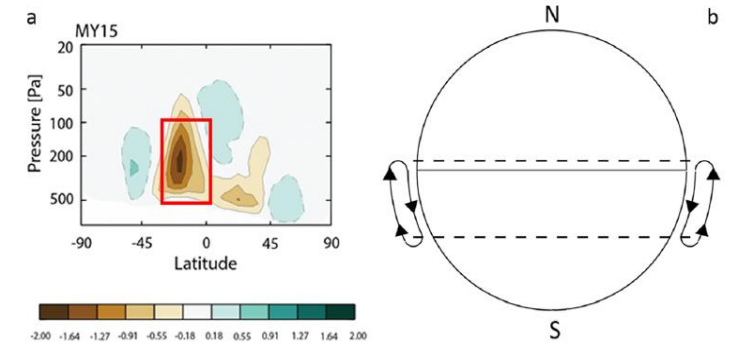
Figure 4. (Not to scale) (a) Meridional stream function differences plot for MY 15 (after Figure 15 of MS17). Units are 10⁻⁹ kg s⁻¹. The boxed area identifies the atmospheric volume that provides parameter values for the modeling performed in this section. (b) System diagram for the flywheel model employed for calculations. Arcs with arrows identify a global-scale meridional overturning circulation cell extending between 4°N and 30°S latitude, corresponding to the span in latitude of the box shown in panel (a). Dashed lines indicate that the circulation shown completely encircles the planet.

(Shirley et al, 2020)

The proposed **"flywheel effect"** has already been simulated and studied in GCM investigations for Mars ^

- Torque reversals may impact the large-scale circulation by interfering destructively with existing circulations

- Continuously varying meridional flow speeds, and cell morphologies, are an expected result

A meridional circulations 'flywheel effect' could plausibly account for the lagging behavior of the solar dynamo during 5-body orbital motion intervals

(Zhao et al. 2013)

The Period of the Hale Cycle During The Most Recent 'Jose Cycle' (1772-1951)

The 9 barycentric orbit cycles from 1772-1951 (of mean period 19.87 yr)
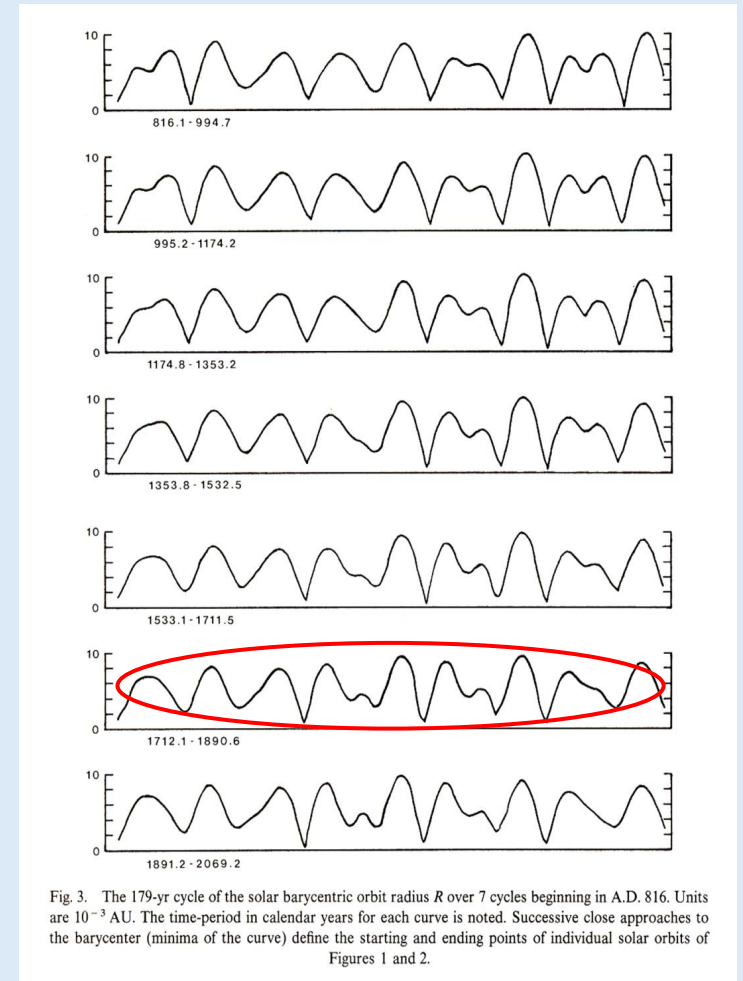were accompanied by 8 Hale magnetic cycles of mean period **22.36 yr**.

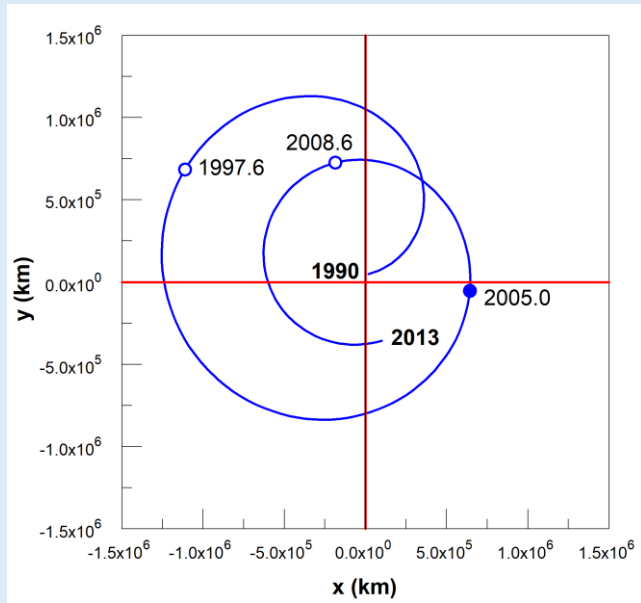| Peribac	Cycle Time	Hale Start Date	Cycle Time
1772.582			
	23.568	1775.538	
1796.150			22.833
	15.283	1798.371	
1811.433			25
	23.666	1823.371	
1835.099			20.167
	15.781	1843.538	
1850.879			23.504
	22.693	1867.042	
1873.573			23.081
	17.553	1890.123	
1891.126			22.501
	21.191	1912.624	
1912.317			21.334
	17.382	1933.958	
1929.699			20.497
	21.679	1954.455	
1951.378			
Cycle Means:	19.866		22.365
σ:	(± 3.36)		(± 1.62)

The system of the four giant planets dictates the decadal-timescale variability of the solar motion

While the orbital dynamics is subject to some long-period variability, the alternation of 3- and 5-body forcing modes is a "built in" repetitive feature

Fun fact: Of the 20 most significant solar prolonged minima recorded over the past 9400 yr, **none occurred during 3-Body motion episodes** (McCracken et al., 2014)

We propose that the fundamental 22+ yr Hale magnetic cycle is driven by giant planet motions through the physical agency of orbit-spin coupling

Fig. 3. The 179-yr cycle of the solar barycentric orbit radius *R* over 7 cycles beginning in A.D. 816. Units are 10^{-3} AU. The time-period in calendar years for each curve is noted. Successive close approaches to the barycenter (minima of the curve) define the starting and ending points of individual solar orbits of Figures 1 and 2.

Fairbridge, R. W., and Shirley, J. H. 1987. Solar Physics 100, 191.

^ The Sun's inward trajectory is interrupted between 2005-2008.6, resulting in reduced torque amplitudes in this interval >

The unusually quiet Schwabe Cycle 23-24 minimum coincides with a multiyear minimum of the torque

A Closer Look at the 5-Body Mode:
(A Case Study of Cycle 23)

Dynamical and magnetic cycles are *out of phase* in Cycle 23
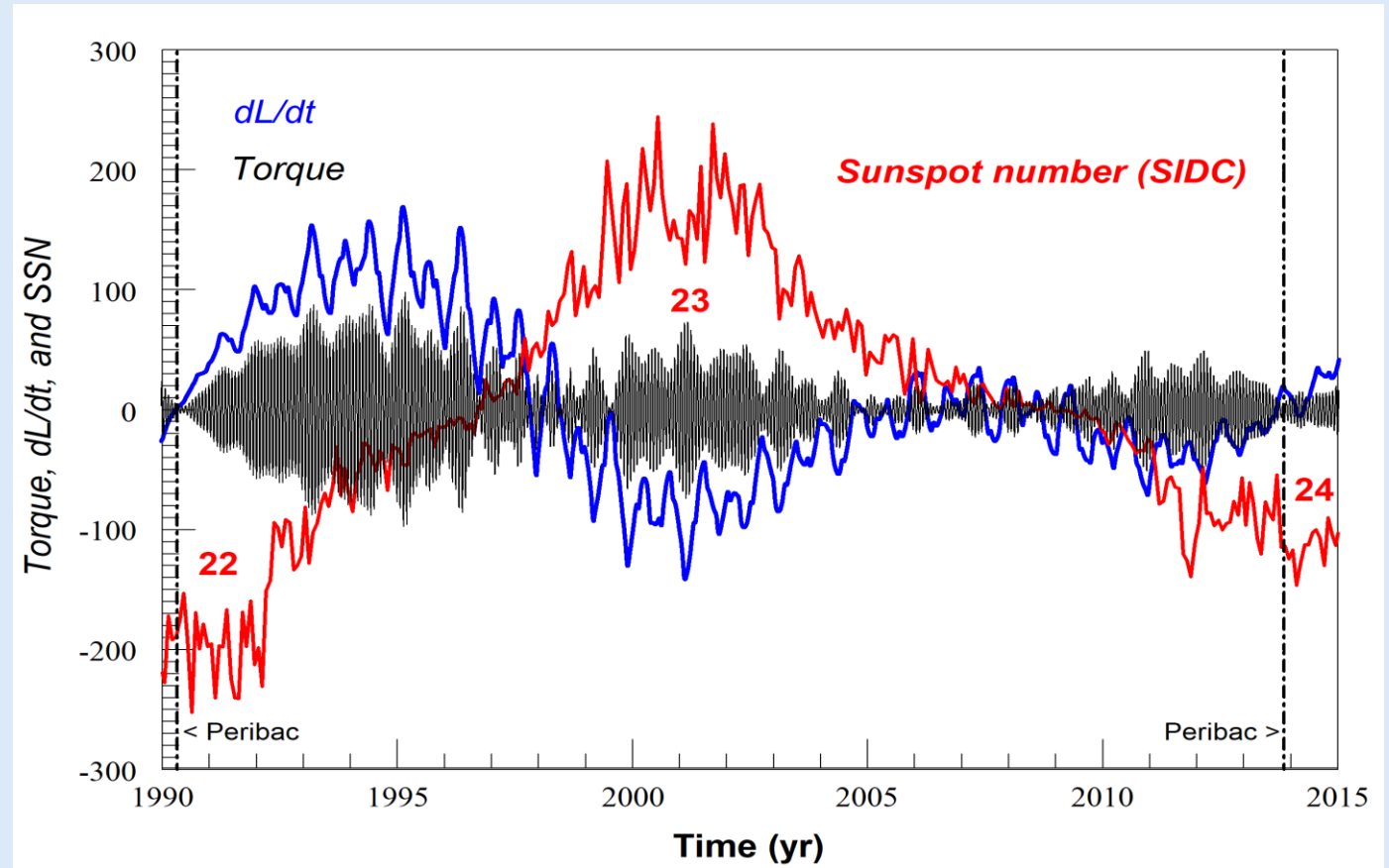
Observed phase relationships hint that the low peak SSN of Cycle 24 may be due to a form of *destructive interference* in Cycle 23

Cycle 23 (continued)

"We perform kinematic solar dynamo simulations to investigate whether internal meridional flow variations can produce deep minima between cycles in general, and, in particular, explain the observed characteristics of the minimum of cycle 23 - a comparatively weak dipolar field strength and an unusually long period without sunspots."

"We therefore perform dynamo simulations by randomly varying the meridional flow speed between 15 and 30ms (with the same amplitude in both the hemispheres) at the solar cycle maximum, and study its effect on the nature of solar cycle minima."

"... a fast meridional flow in the first half of a cycle, followed by a slower flow in the second half, reproduces both characteristics of the minimum of sunspot cycle 23."

Torque amplitudes in the first half of Cycle 23 are larger than those of the second half by a factor of 2.5

LETTER

doi:10.1038/nature09786

The unusual minimum of sunspot cycle 23 caused by meridional plasma flow variations
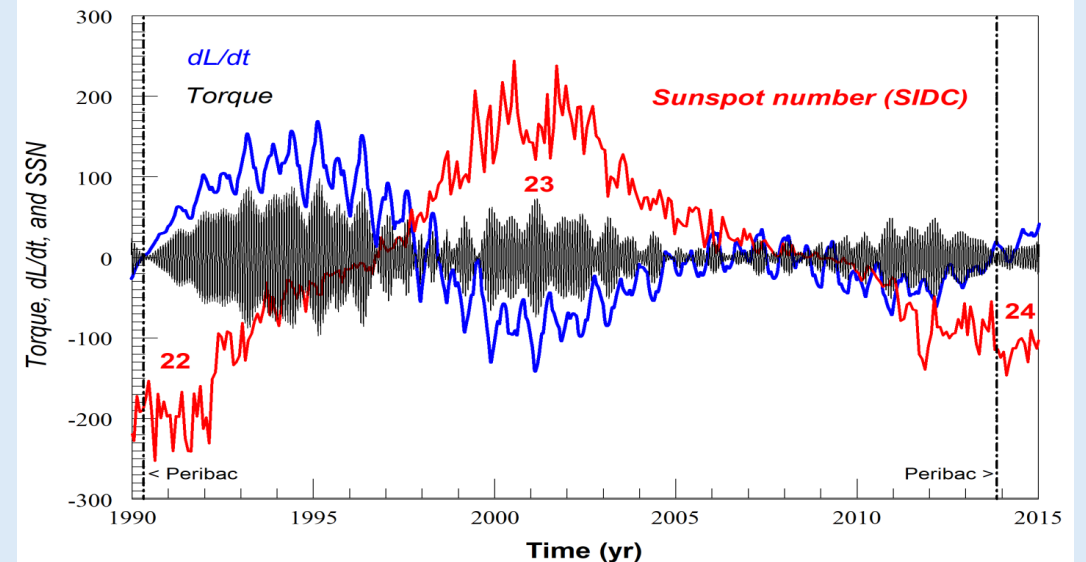
Dibyendu Nandy[1], Andrés Muñoz-Jaramillo[2,3] & Petrus C. H. Martens[2,3]

Direct observations over the past four centuries[1] show that the number of sunspots observed on the Sun's surface varies periodically, going through successive maxima and minima. Following sunspot cycle 23, the Sun went into a prolonged minimum characterized by a very weak polar magnetic field[2,3] and an unusually large number of days without sunspots[4]. Sunspots are strongly magnetized regions[5] generated by a dynamo mechanism[6] that recreates the solar polar field mediated through plasma flows[7]. Here we report results from kinematic dynamo simulations which demonstrate that a fast meridional flow in the first half of a cycle, followed by a slower flow in the second half, reproduces both characteristics of the minimum of sunspot cycle 23. Our model predicts that, in general, very deep minima are associated with weak polar fields. Sunspots govern the solar radiative energy[8,9] and radio flux, and, in conjunction with the polar field, modulate the solar wind, the heliospheric open flux and, consequently, the cosmic ray flux at Earth[3,10,11].

meridional flow speed between 15 and 30 m s^{−1} (with the same amplitude in both the hemispheres) at the solar cycle maximum, and study its effect on the nature of solar cycle minima. Details of the dynamo model are described in Supplementary Information.

Our simulations extend over 210 sunspot cycles corresponding to 1,860 solar years; for each of these simulated cycles, we record the meridional circulation speed, the cycle overlap (which includes the information on the number of days with no sunspots) and the strength of the polar radial field at cycle minimum. Figure 1 shows the sunspot butterfly diagram and surface radial field evolution over a selected 40-yr slice of the simulation. Here cycle to cycle variations (mediated by varying meridional flows) in the strength of the polar field at minimum and the structure of the sunspot butterfly diagram are apparent, hinting that the number of spotless days during a minimum is governed by the overlap (or lack thereof) of successive cycles.

We designate the minimum in activity following a given sunspot cycle, say n, as the minimum of n (because the sunspot eruptions from

Time Delay Effects and System Memory (2)

NSSL magnetic phenomena lag time ~ 4 months >

< Cycle 23-24: Suggested lag time ~ a few years

The unusual minimum of sunspot cycle 23 caused by meridional plasma flow variations

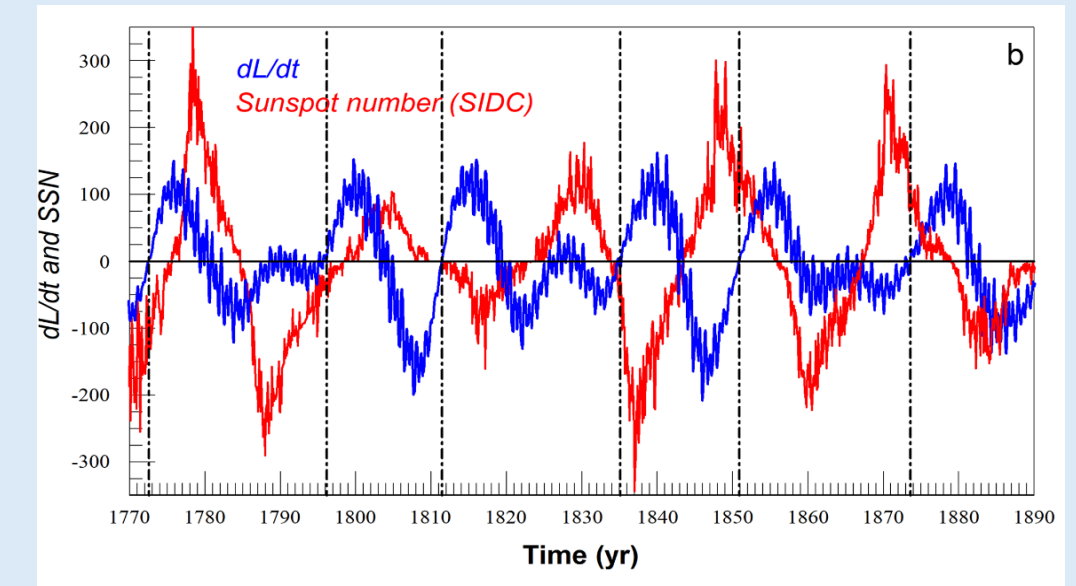Dibyendu Nandy[1], Andrés Muñoz-Jaramillo[2,3] & Petrus C. H. Martens[2,3]

Direct observations over the past four centuries[1] show that the number of sunspots observed on the Sun's surface varies periodically, going through successive maxima and minima. Following sunspot cycle 23, the Sun went into a prolonged minimum characterized by a very weak polar magnetic field[2,3] and an unusually large number of days without sunspots[4]. Sunspots are strongly magnetized regions[5] generated by a dynamo mechanism[6] that recreates the solar polar field mediated through plasma flows[7]. Here we report results from kinematic dynamo simulations which demonstrate that a fast meridional flow in the first half of a cycle, followed by a slower flow in the second half, reproduces both characteristics of the minimum of sunspot cycle 23. Our model predicts that, in general, very deep minima are associated with weak polar fields. Sunspots govern the solar radiative energy[8,9] and radio flux, and, in conjunction with the polar field, modulate the solar wind, the heliospheric open flux and, consequently, the cosmic ray flux at Earth[3,10,11].

meridional flow speed between 15 and 30 m s^{-1} (with the same amplitude in both the hemispheres) at the solar cycle maximum, and study its effect on the nature of solar cycle minima. Details of the dynamo model are described in Supplementary Information.

Our simulations extend over 210 sunspot cycles corresponding to 1,860 solar years; for each of these simulated cycles, we record the meridional circulation speed, the cycle overlap (which includes the information on the number of days with no sunspots) and the strength of the polar radial field at cycle minimum. Figure 1 shows the sunspot butterfly diagram and surface radial field evolution over a selected 40-yr slice of the simulation. Here cycle to cycle variations (mediated by varying meridional flows) in the strength of the polar field at minimum and the structure of the sunspot butterfly diagram are apparent, hinting that the number of spotless days during a minimum is governed by the overlap (or lack thereof) of successive cycles.

We designate the minimum in activity following a given sunspot cycle, say n, as the minimum of n (because the sunspot eruptions from

~120 yr 5-Body Hale Cycles cumulative lag: ~ one Hale Cycle >
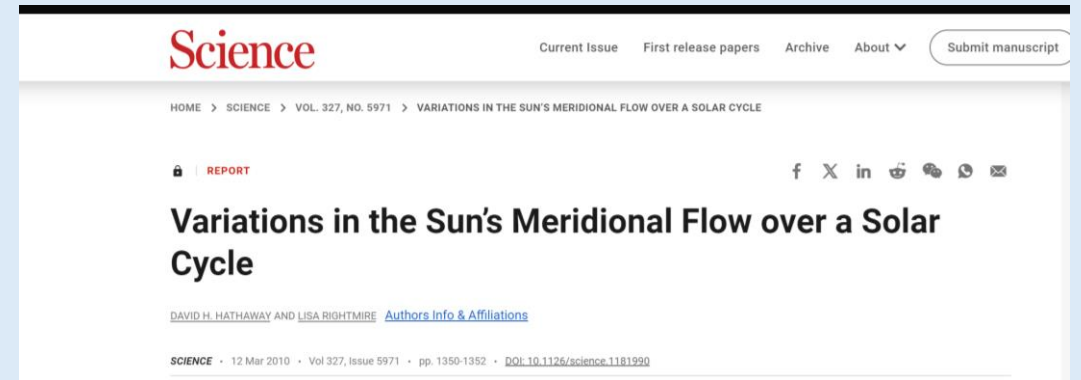
On the Anti-Correlation of Meridional Flow Speeds and Sunspot Cycle Activity Levels

Early investigations of flux transport dynamo models suggested that meridional flow speeds and magnetic cycle activity levels should be *positively* correlated

The orbit-spin coupling hypothesis predicts that larger torque amplitudes should give rise to stronger effects on meridional accelerations, and is consistent with the expectation above

Direct observations of meridional flow speeds however reveal an anti-correlation of flow speeds and activity levels over the past few cycles. Modelers must now take account of this constraint.

Increasing torques in out-of-phase conditions, as in Cycle 23, may destructively interfere with existing large-scale flows, potentially leading to *suppressed* magnetic activity, and to observations of slower near-surface meridional flow speeds near activity maxima, as shown in Hathaway and Rightmire (2010)
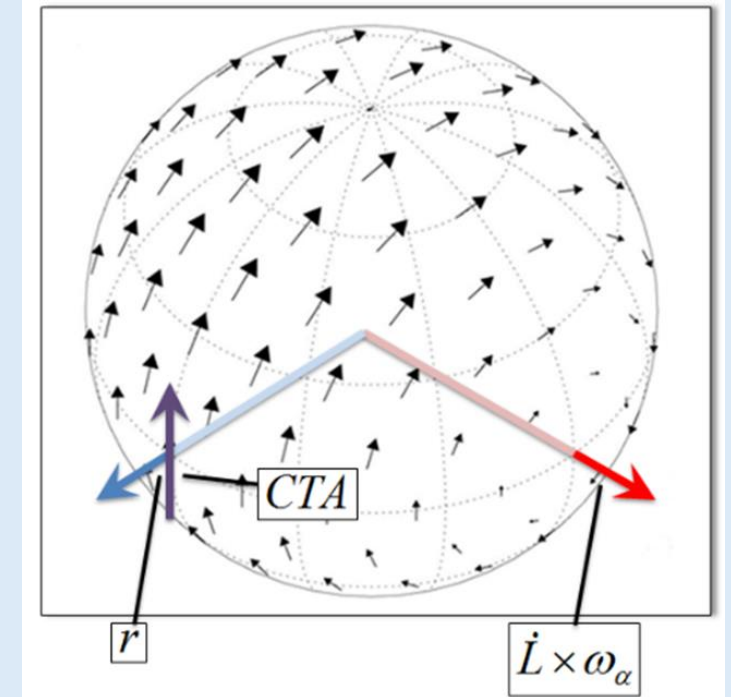

We suspect that *positive correlations* would be obtained if the period analyzed fell within a 3-body motions interval (as in 1891-1951)

The Next Two Hale Cycles

- The next 3-body motions episode begins late in 2069

- We expect that the phases of the dynamical and magnetic cycles will then return to synchronization

- Two complete Hale Cycles should be completed in the years 2019.9 – 2070

- The current (25) and upcoming three Schwabe Cycles (26, 27, 28) will on average be **longer than 11 yr in duration**

| Peribac	Cycle Time	Hale Start Date	Cycle Time
1951.378			
	23.822	1954.455	
1975.200			22.085
	15.110	1976.540	
1990.310			20.169
	23.548	1996.709	
2013.858			23.249
	16.210	2019.958	
2030.068			24.5?
	22.033	2044.5?	
2052.101			24.5?
	17.888	2069?	
2069.989			
	19.769 +/- 3.84		23.10 +/- 1.82
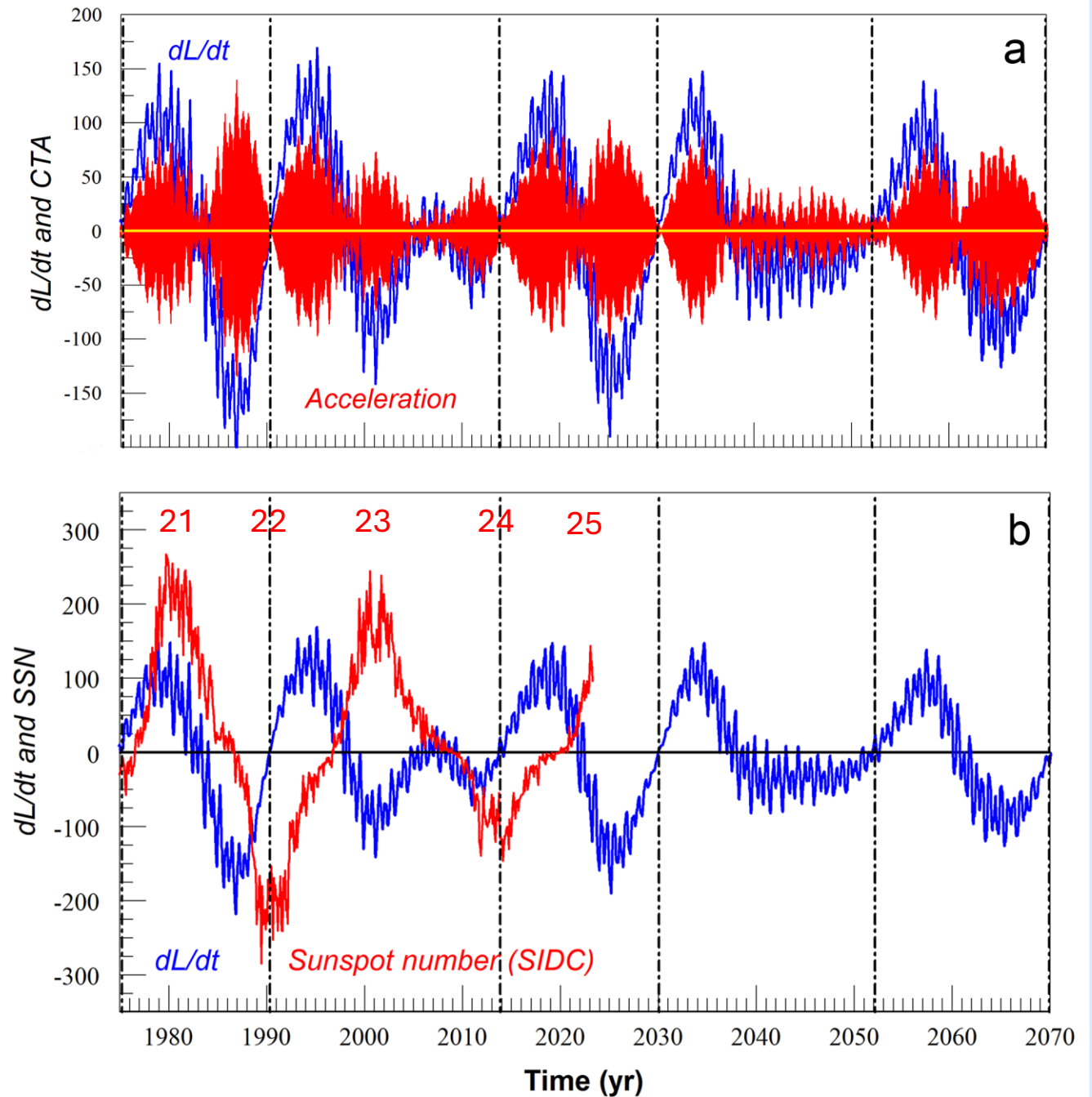
Open questions, and key role, of large-scale flows:

"Current simulations struggle to reproduce solar convection and the resulting differential rotation at the solar luminosity and rotation rate." (the "convective conundrum")

"Given the difficulties in reproducing the solar flows, it is then hardly surprising that dynamo simulations have a hard time reproducing the large-scale solar magnetism."

"...the solar velocity field has to be sufficiently well reproduced first before one should expect success in reproducing the dynamo."

(From: Käpylä et al., 2023, Simulations of solar and stellar dynamos and their theoretical interpretation, Space Science Reviews 219:58 (2023)

Can better agreement of simulations with observations be achieved by including orbit-spin coupling contributions to flow velocities in MHD dynamo models?
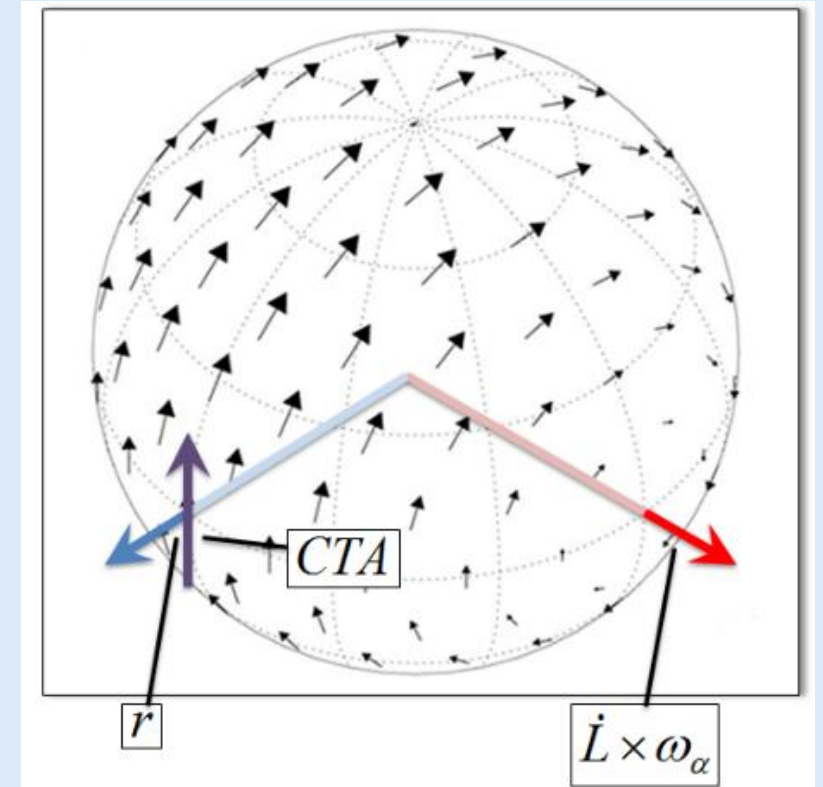
Summary and Conclusions

- Orbit-spin coupling for the first time offers a testable, fully deterministic physical explanation for the observed time variability of Hale and Schwabe cycle periods since the end of the Maunder Minimum

- We propose that the solar barycentric orbital revolution, with orbital cycle times ranging from ~15 yr to ~25 yr, and mean of 19.86 yr, is ultimately responsible for setting the timing of the solar dynamo

- The long-term-mean Hale magnetic cycle period of ~22+ yr results from a lagging of the magnetic cycle, with respect to solar barycentric orbital cycle times, due to time-delay effects, occurring mainly during 5-body solar motion episodes.

Thank you!

Algorithms and data employed are available on request from the author
jrocksci@att.net
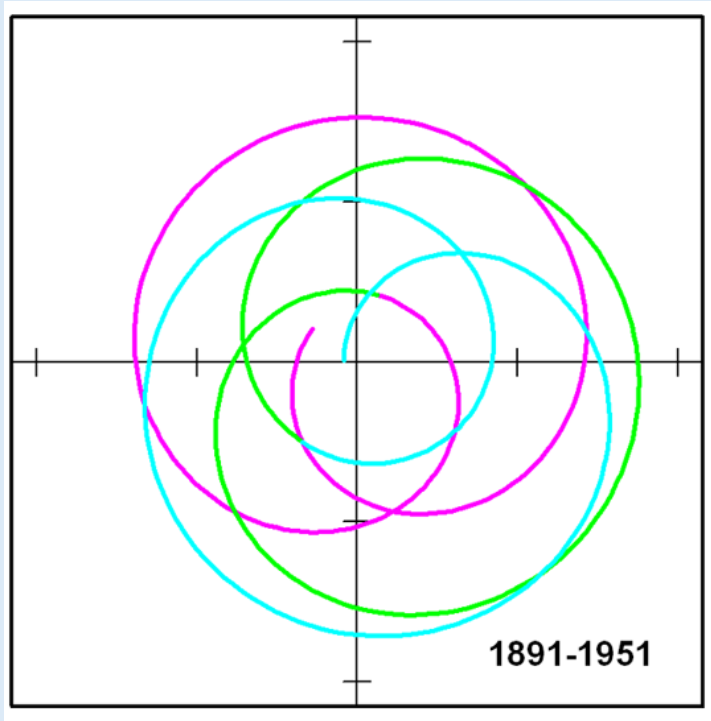
Backup Slides
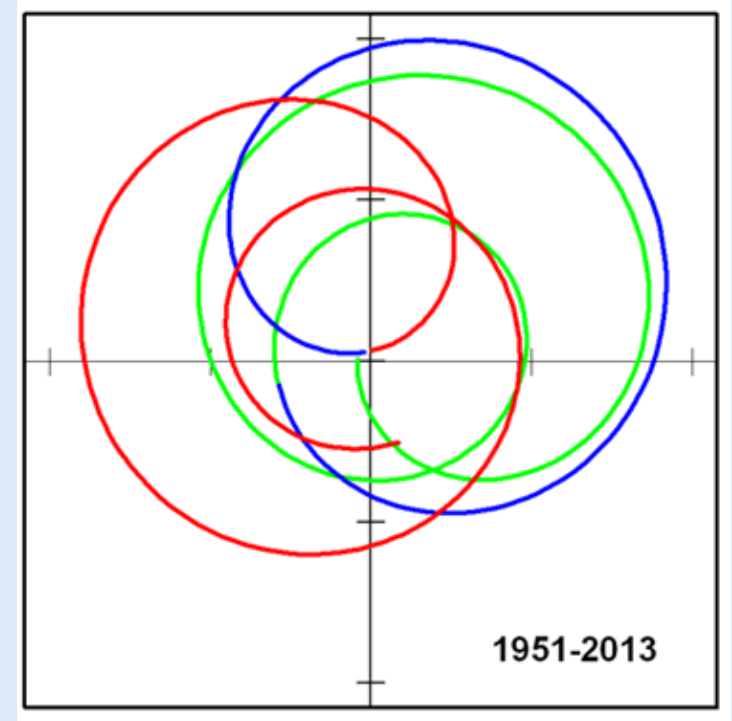
2.3.3. Preliminary estimate of orbit-spin coupling acceleration magnitudes for the Sun

We first obtain dL/dt as a function of time, with respect to the solar system barycenter, referenced to the J2000 ecliptic coordinate system. Peak values of dL/dt, during the time period analyzed, were achieved on 13 November 1986. We obtain Cartesian components (**x, y, z**) of dL/dt of [-4.0487, -3.0299, -2.1655 x 10^2] for that date, in units of m^2 s^{-2} M_{Sun}.

We next resolve the vector angular velocity of the mean solar sidereal rotation $\boldsymbol{\omega_a}$ (employing rotational elements from Beck and Giles, 2005) in the same Cartesian ecliptic coordinate frame, obtaining components of [3.422 x 10^{-7}, -1.013 x 10^{-7}, 2.843 x 10^{-6}] (all in radians per second). The cross product of these vectors yields $\boldsymbol{\dot{L}} \times \boldsymbol{\omega_a}$ = [5.0659 x 10^{-5}, -4.8542 x 10^{-5}, -1.5164 x 10^{-12}], now with temporal units of s^{-3}. We obtain the product of this with $\boldsymbol{r}$ (for a location on the Sun's surface), using a value of $\boldsymbol{r}$ = [6.96 x 10^8 m, 0, 0]. We obtain a vector of magnitude 4.8824 x 10^4 from the above operations. To obtain the associated surface tangential acceleration (i.e., with temporal units of s^{-2}), we employ methods described in Appendix B, which take account of the freely-falling nature of the Sun's motion with respect to the barycenter (Shirley, 2006), retaining only that portion that is varying from one time step to the next. We obtain a value of 4.8824 x 10^4 m s^{-2} for the effective surface acceleration of the couple when c = 1.

To complete the calculation, we are required to supply a value for c. Values of the coupling coefficient c are best determined through comparisons of numerical simulations with observations (Shirley, 2017a; Mischna and Shirley, 2017). In advance of any form of solar numerical modeling, we here employ a c value that was previously optimized for Mars, i.e., 5.0 x 10^{-13}, as our current best estimate (CBE). (Any other choice, at this point, would require us to introduce and justify additional assumptions. Our use of the Mars c value is more likely to be conservative than to be overly aggressive, as the physical properties and relative physical dimensions of the solar convection zone, and tachocline, differ significantly from those of the shallow and tenuous Martian atmosphere).

We obtain a peak tangential acceleration at the Sun's surface of 2.44 x 10^{-8} m s^{-2} with c = 5.0 x 10^{-13}. The corresponding estimate at the depth of the tachocline is 1.71 x 10^{-8} m s^{-2}. These values are larger than the peak tidal acceleration of Jupiter, at perihelion, for the corresponding locations, by factors of 66 and 57 respectively.

2. FUNDAMENTALS OF MAGNETOHYDRODYNAMICS

Physical conditions in the solar interior up to the photosphere are such that the interaction of fluid flow and magnetic field is well-described by the magnetohydrodynamical approximation (hereafter MHD; see, e.g., Davidson 2001). In its classical formulation, MHD describes the behavior of an electrically neutral mixture of electrically charged microscopic constituents in which the collision frequency largely exceeds any relevant plasma frequencies. In such a (moving) collisionally dominated plasma, Ohm's law holds in a reference frame comoving with the fluid at the macroscopic scale. For a nonrelativistic fluid flow $\mathbf{u}$, the rest frame electric field $\mathbf{E}$ is then simply

$$\mathbf{E} = \mathbf{J}/\sigma - \mathbf{u} \times \mathbf{B}, \tag{1}$$

where $\mathbf{J}$ and $\mathbf{B}$ are, respectively, the current density and magnetic field, and σ is the electrical conductivity (SI units are used throughout). Excluding externally imposed rapid variations of $\mathbf{E}$ (e.g., turning batteries on or off), Ampère's law holds in its pre-Maxwellian form,

$$\nabla \times \mathbf{B} = \mu_0 \mathbf{J}, \tag{2}$$

where μ_0 is the magnetic permeability. Using this expression to substitute for $\mathbf{J}$ in Equation 1 and inserting the resulting expression for $\mathbf{E}$ into Faraday's law leads to the MHD induction equation,

$$\frac{\partial \mathbf{B}}{\partial t} = \nabla \times (\mathbf{u} \times \mathbf{B} - \eta \nabla \times \mathbf{B}), \tag{3}$$

Time-Delay Effects and System Memory (3)

The differences between the magnetic cycle responses to the 3-body and 5-body modes may be interpreted in terms of a simple oscillatory model such as a child on a swing. In-phase resonant forcing during 3-body intervals results in secular strengthening of the dynamo. Rapidly changing, out-of-phase forcing during 5-body episodes effects a sort of destructive interference, yielding stronger cycle amplitude variability and more irregular cycle times.

Meridional flow cells possess inertia and have been identified as a source of memory for the dynamo. Their flows cannot respond instantaneously to rapidly changing forcing. Hence the observed lagging of the magnetic cycle, with respect to the dynamical cycle, during 5-body episodes may be plausibly attributed to a meridional flows "flywheel effect" as already documented for Mars

Could orbit-spin coupling torques give rise to torsional oscillations?

(d) Hemispherically Averaged SOHO/MDI Differential Rotation Residual at 0.993 Rsun
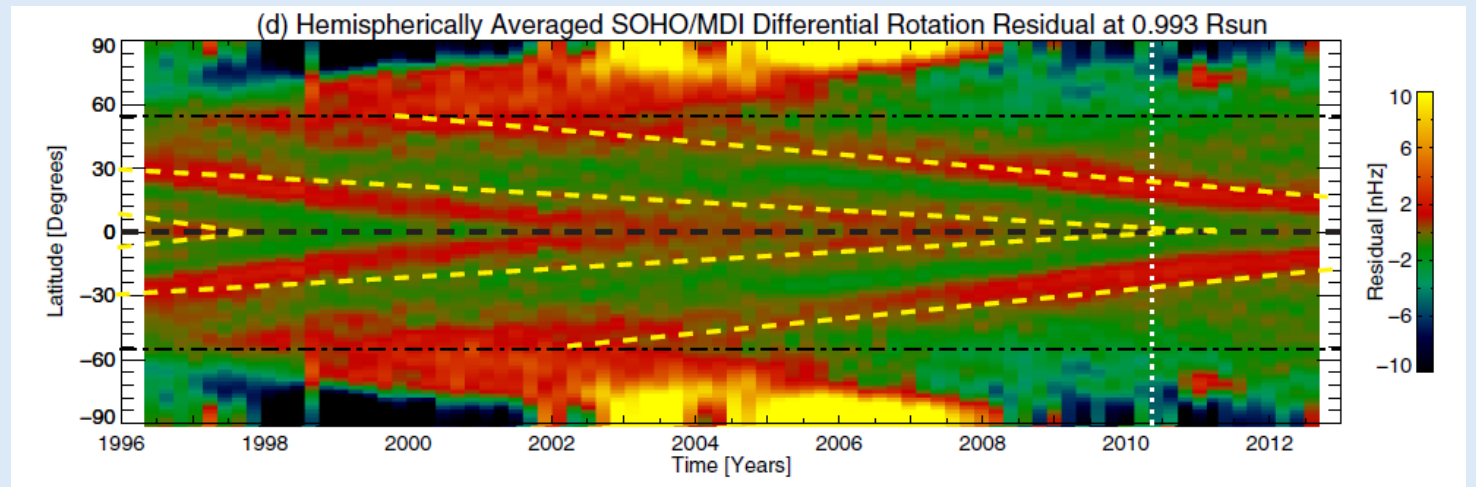
The 'torsional oscillations' are bands of faster than average and slower than average *zonal* motions within the solar convective zone. They bracket the latitudes of solar active regions, and extend to great depths within the CZ. Zonal velocity differences are about +/- 5-10 m s^{-1} or +/- 0.5%. Yellow lines describe the migration of activity bands with time (McIntosh et al. 2014)

Inner Planet Contributions

Pulsations of the torque amplitude occur nearly continuously, in association with the variability of dL/dt driven by inner planet motions

While large-scale flows at depth may primarily vary due to torques acting on decadal timescales, near-surface regions, with lower inertia, may have shorter response times

Complex, high-frequency changes in dynamical forcing may thus engender electromagnetic signatures corresponding to inner planet periods and beat frequencies, as detected in irradiance records
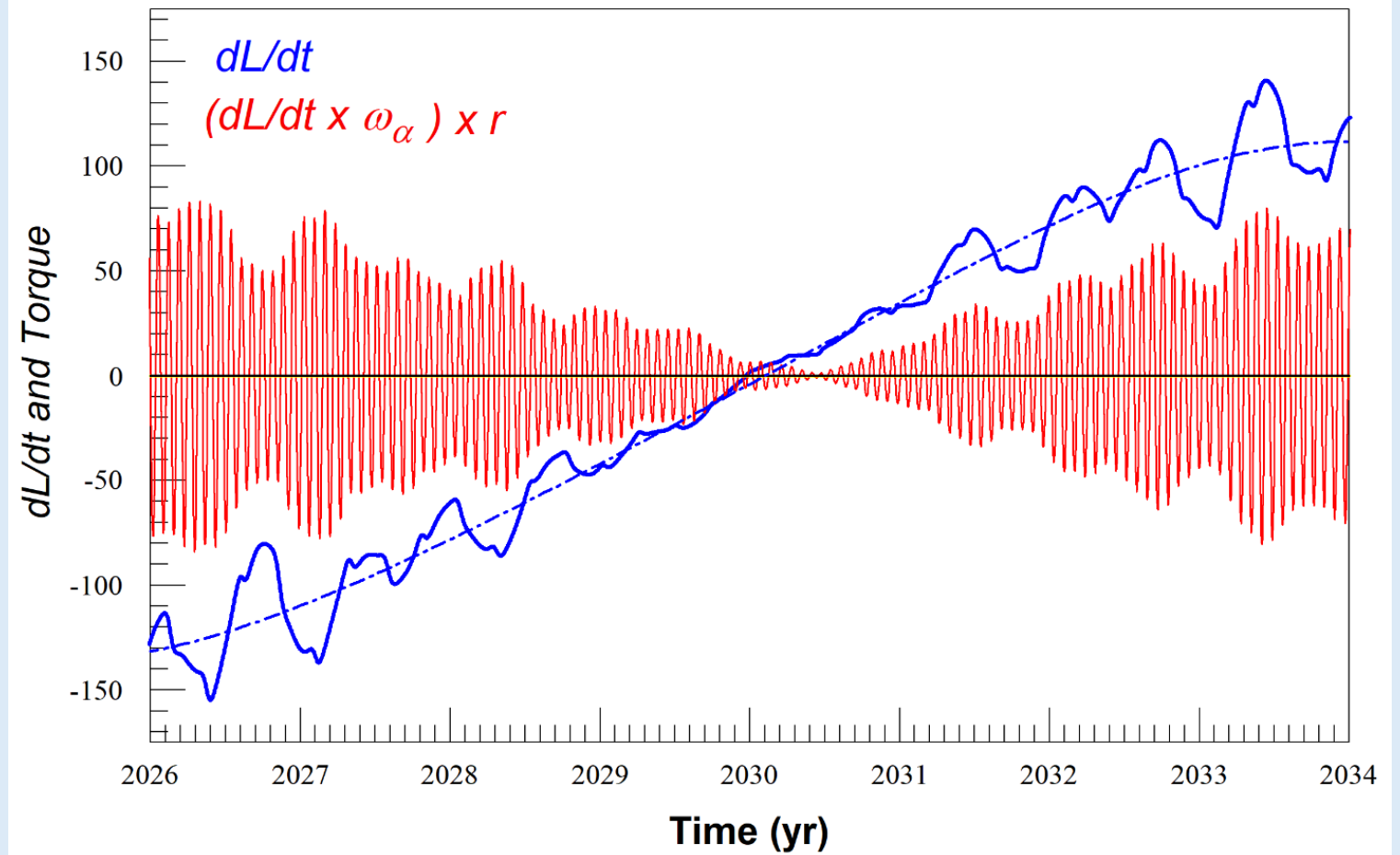
The solid blue curve gives the (dominant) ecliptic-frame **z** component of the vector valued forcing function (*dL/dt*) for the Sun. Giant planet contributions (dashed-dotted curve) account for the long-period modulation. Units of *dL/dt* are $m^2 \, s^{-2} \, M_{Sun}$ (i.e., the unit of mass is the solar mass of 1.99×10^{30} kg). Scaled contemporaneous tangential surface coupling term accelerations (*cta*) for one particular heliographic location on the Sun are illustrated in red. Here each oscillation of upward (northward) and downward (southward) acceleration corresponds to one standard 25.38 d period of rotation of the heliographic coordinate system. Data (at 1-d time steps) for the solid blue curve, and for the accelerations curve in red, are extracted from the JPL Development Ephemeris DE-441.
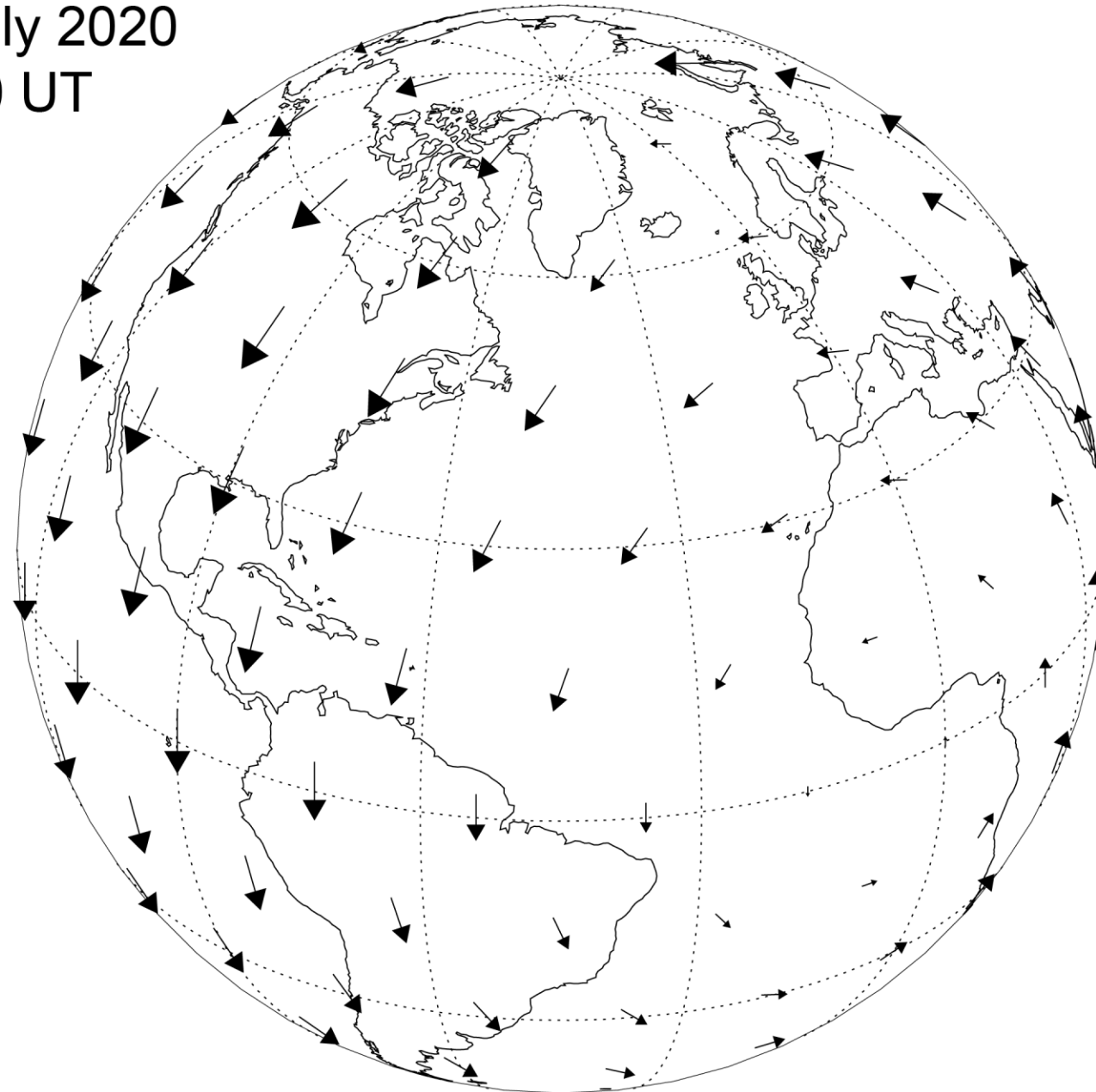
Carrington-timescale azimuthal cycling

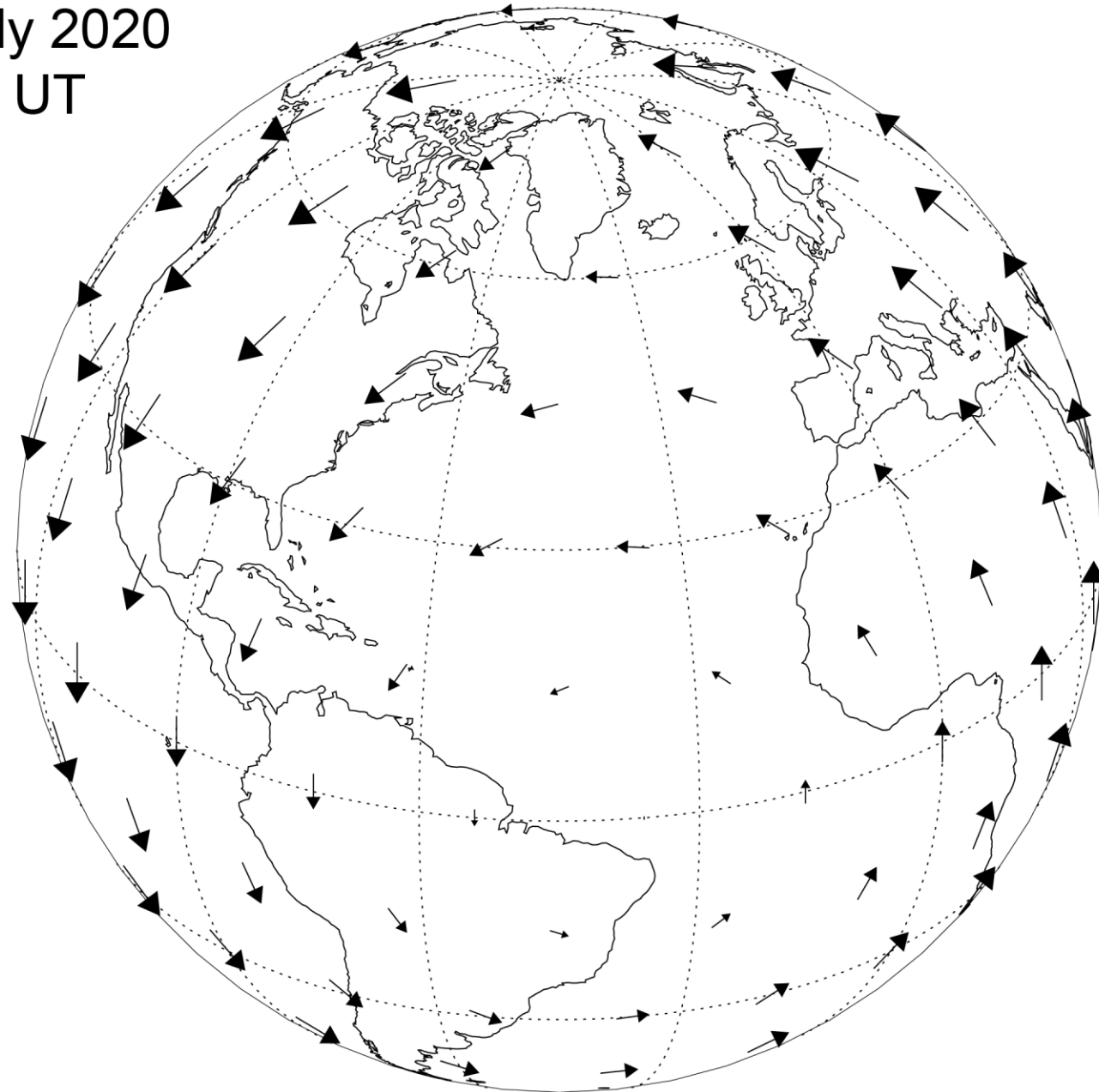(Using an example depicting Earth rotation)
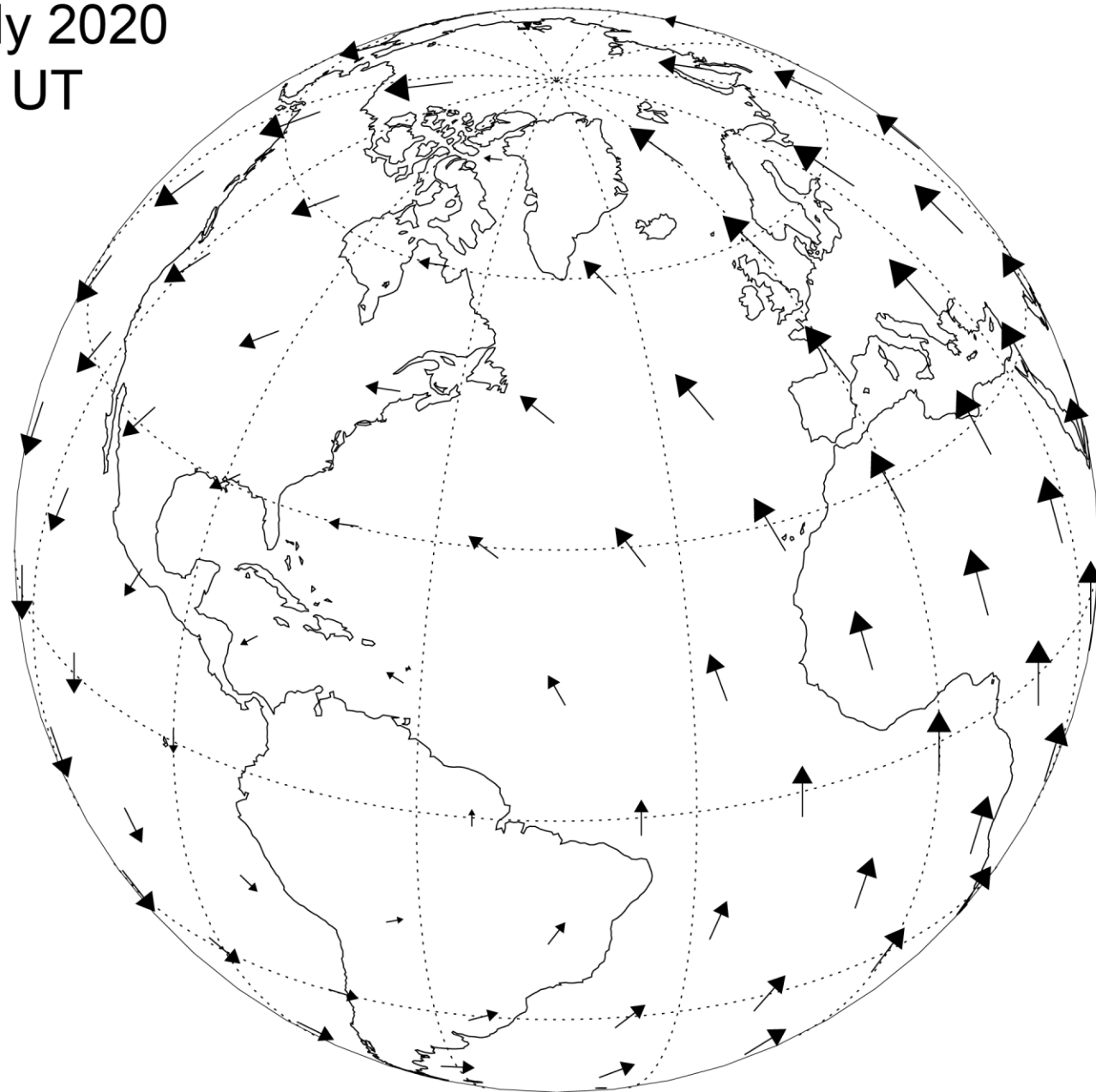
26 July 2020
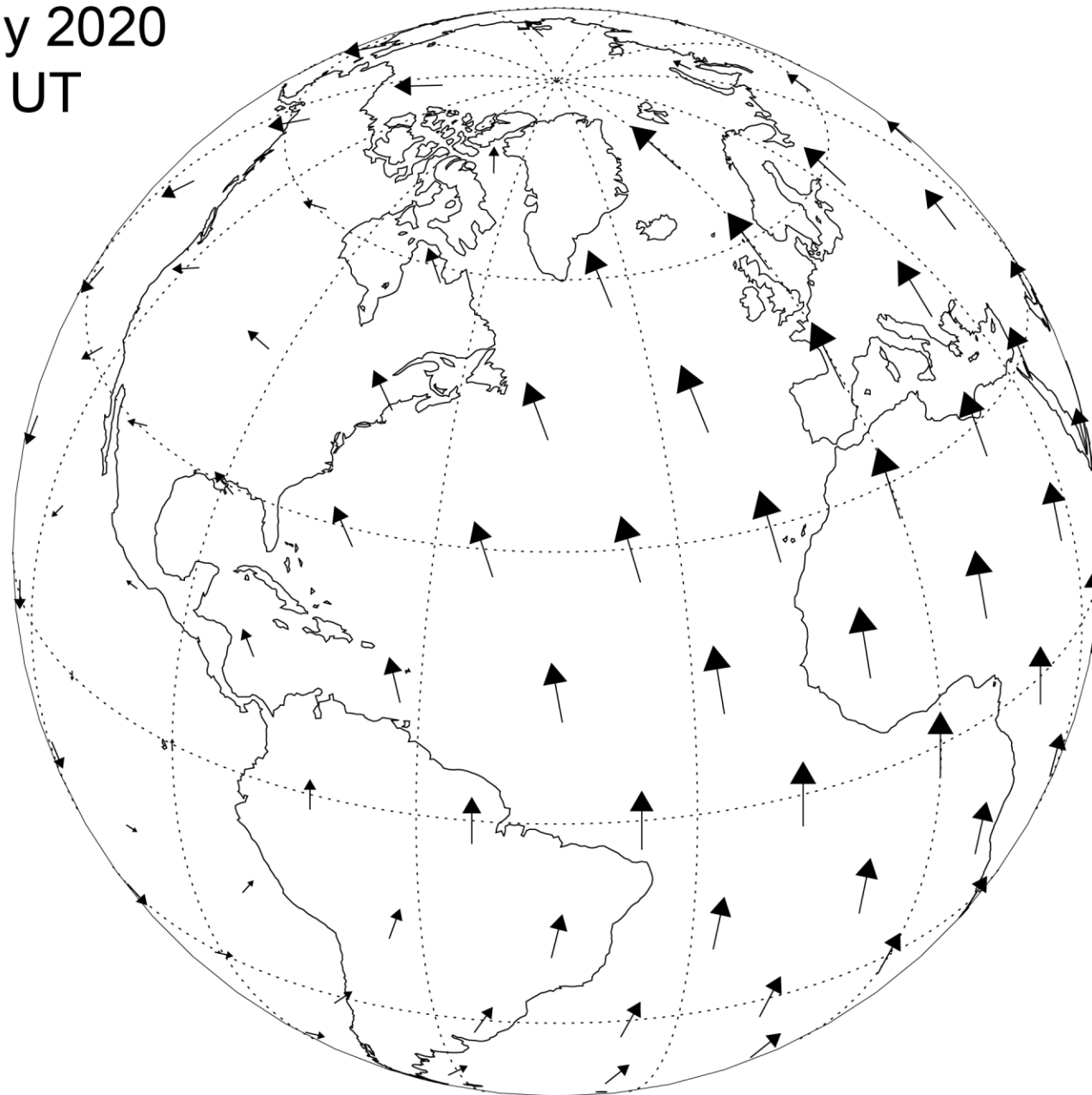21:00 UT
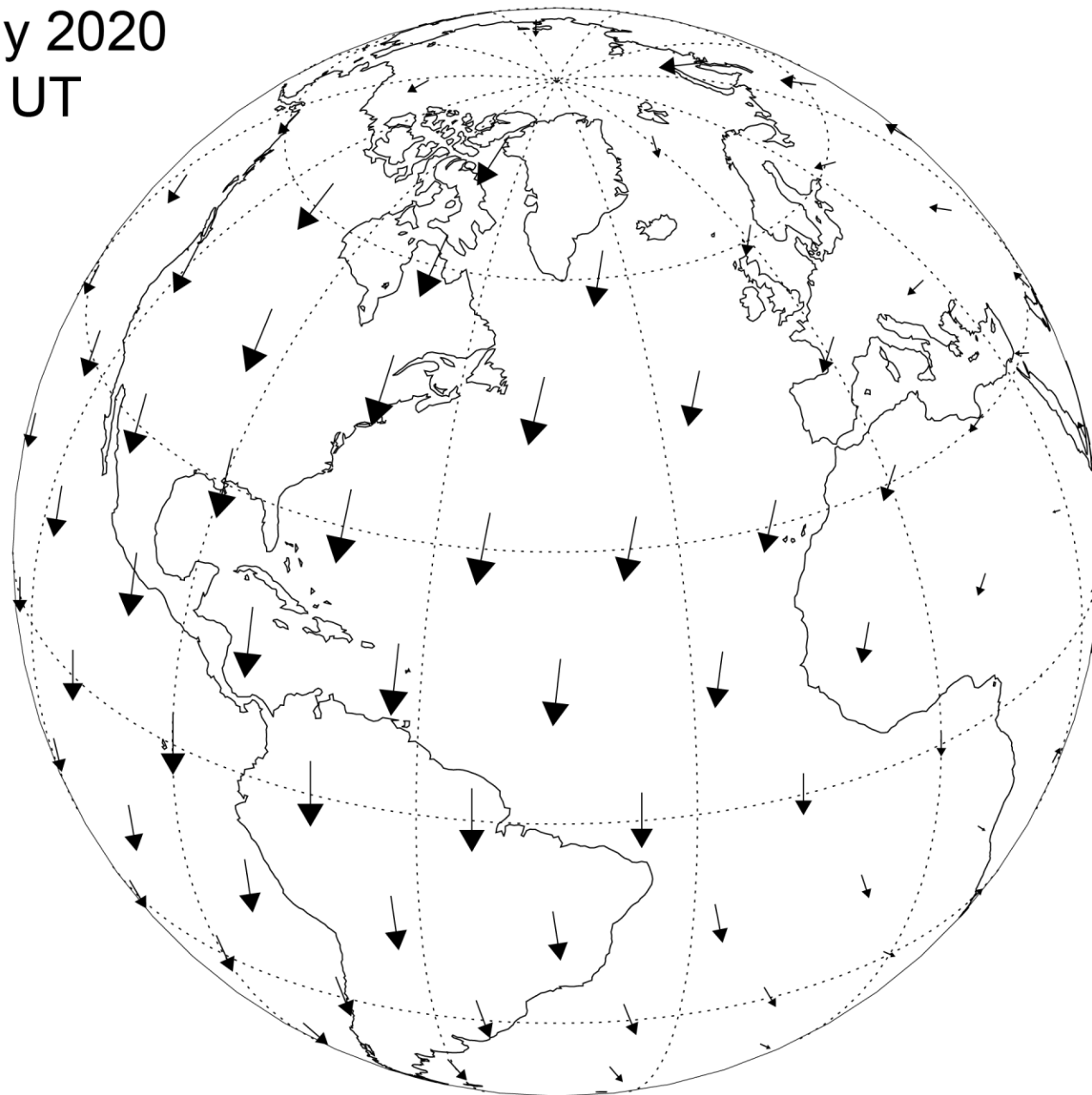
26 July 2020
23:00 UT

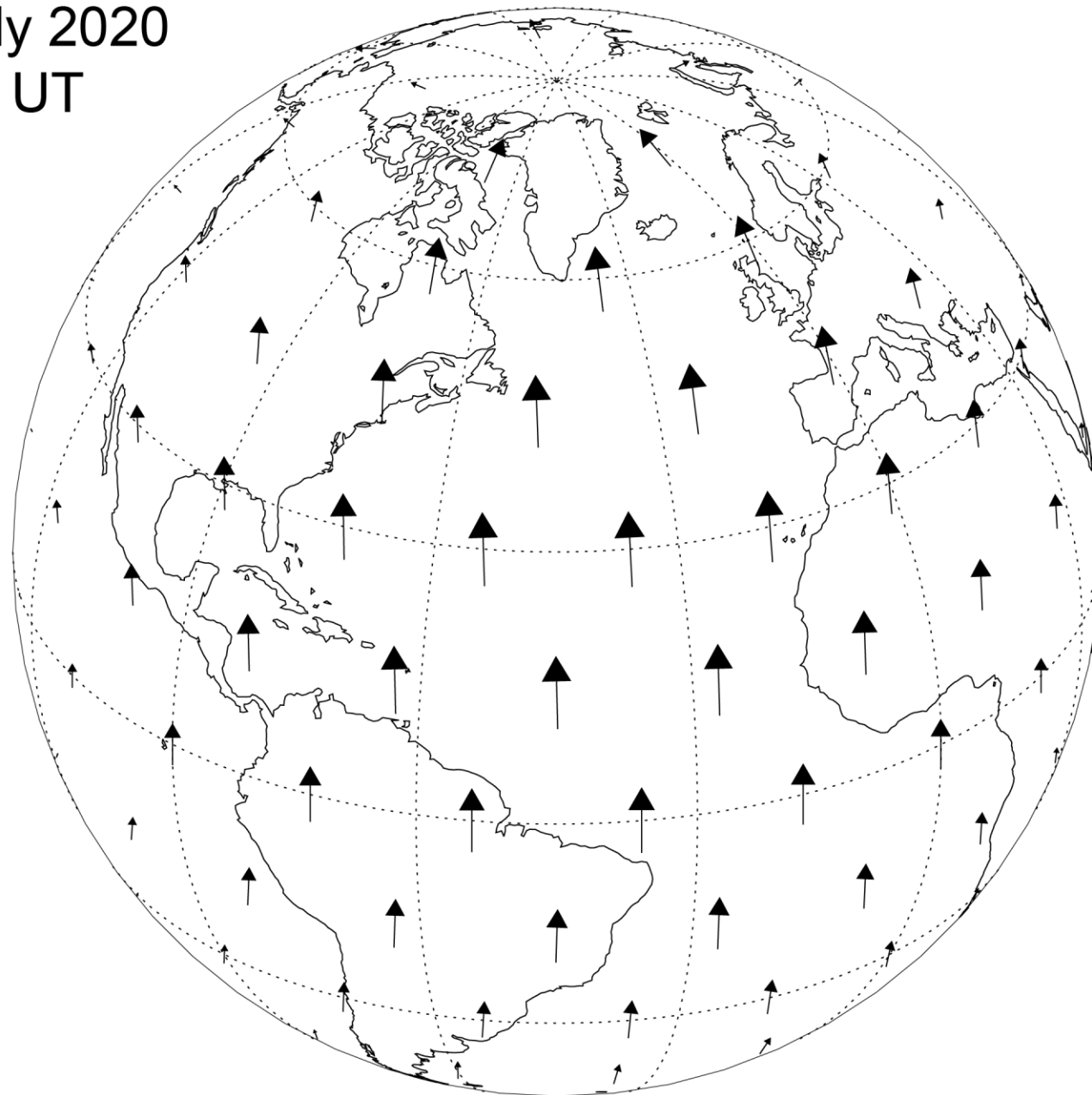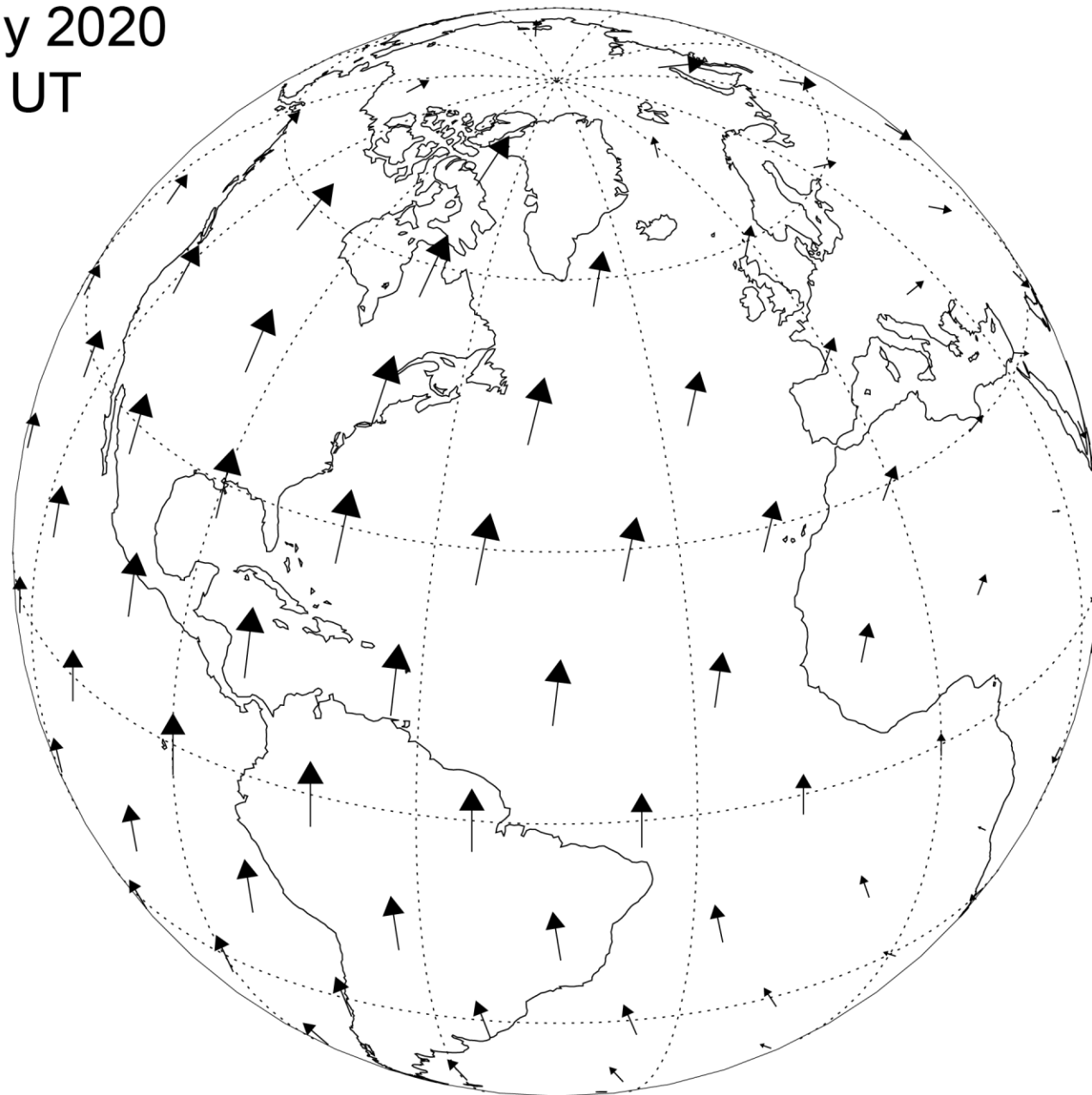27 July 2020
01:00 UT

27 July 2020
03:00 UT

27 July 2020
05:00 UT

27 July 2020
07:00 UT

27 July 2020
09:00 UT

Orbit-Spin Coupling

- An equation describing a weak coupling of the orbital and rotational motions is derived in *Shirley* (2017)

- The physical hypothesis predicts a strong modulation with time of large-scale flows in extended-body atmospheres

- Global Circulation Modeling by Mischna & Shirley (P&SS 141, 45) replicates conditions favorable for the occurrence of global dust storms on Mars in the years in which such storms actually occurred

Orbit-spin coupling and the circulation of the Martian atmosphere[*]

James H. Shirley

Jet Propulsion Laboratory, California Institute of Technology, Pasadena, CA, USA

ARTICLE INFO

ABSTRACT

The physical origins of the observed interannual variability of weather and climate on Mars are poorly understood. In this paper we introduce a deterministic physical mechanism that may account for much of the variability of the circulation of the Mars atmosphere on seasonal and longer timescales. We focus on a possible coupling between the planetary orbital angular momentum and the angular momentum of the planetary rotation. We suspect that the planetary atmosphere may participate in an exchange of momentum between these two reservoirs. Nontrivial changes in the circulation of the atmosphere are likely to occur, as the atmospheric system gains and loses angular momentum, during this exchange. We derive a coupling expression linking orbital and rotational motions that produces an acceleration field varying with position and with time on and within a subject body. The spatially and temporally varying accelerations may interfere constructively or destructively with large-scale flows of geophysical fluids that are established and maintained by other means. This physical hypothesis predicts cycles of intensification and relaxation of circulatory flows of atmospheres on seasonal and longer timescales that are largely independent of solar forcing. The predictions of this hypothesis may be tested through numerical modeling. Examples from investigations of the atmospheric circulation of Mars are provided to illustrate qualitative features and quantitative aspects of the coupling mechanism proposed.

iStock #157681467 Credit: Angelika